Deltares

A comparison of two models for consolidation with regard to the potential impact on practice

A comparison of two models for consolidation with regard to the potential impact on practice

Author(s)
Andre Koelewijn

A comparison of two models for consolidation with regard to the potential impact on practice

Client	Rijkswaterstaat Water, Verkeer en Leefomgeving
Contact	Myron van Damme
Reference	Sito-PS KvK 2024
Keywords	Consolidation, porous media, Biot, volumetric strain, alternative formulation

Document control	
Version	1.0
Date	10-12-2024
Project nr.	11210371-028
Document ID	11210371-028-GEO-0002
Pages	17
Classification	
Status	Final

Author(s)		
	Andre Koelewijn	

Summary

The response of water saturated porous media to hydrodynamic loads is an issue of practical relevance to many applications in civil engineering, including many situations at the transition between soil and water. In 1941 Biot published a method to calculate the development of pore pressures in a porous medium, which is now commonly used in the field of geomechanics. Recently, Van Damme and Den Ouden-Van der Horst (2023) published an alternative approach. This report describes a limited investigation of the practical implications of this new approach.

By comparing the results of both models an indication of potential differences is obtained. The comparison was done for cases with various boundary conditions and assuming only compressible pore water.

It is concluded that for the pore pressures the same solution is obtained by both models, yet the deformations may be different, up to a factor of (at least) three, with sometimes an overall different spatial distribution. Due to these differences it cannot be easily determined which of the two models generally resembles reality more closely.

On the basis of this study, it may be inferred that there may be a considerable impact on the accuracy of calculations in various civil engineering applications, where dynamic loads have an important effect. Moreover, yet outside the scope of this study, the new model may impact the practice of undrained analyses for basically transient situations, like stability analyses of embankments or failure analyses of dike revetments.

This would require a more widely scoped investigation, in which the implications of the approach by the new model can also be scrutinized, e.g. regarding the interpretation of laboratory and field tests.

It is therefore recommended that further (fundamental) research is carried out, initially at an academic level, and that results of this research are disseminated into practice as soon as possible, either directly or in cooperation with applied research institutes.

Contents

1 Introduction

The response of water saturated porous media to hydrodynamic loads is an issue of practical relevance to many applications in civil engineering, including many situations at the transition between soil and water.

In 1941 Biot published a method to calculate the development of pore pressures in a porous medium, which is now commonly used in the field of geomechanics. Recently, Van Damme and Den Ouden-Van der Horst (2023) published an alternative approach, imposing different boundary conditions than Biot. Most notably, the effective stress principle of Terzaghi, stating that the effective stresses at the surface of porous medium are zero, is abandoned. The recent article indicates that this is an unnecessary assumption.

After some debate, Rijkswaterstaat gave an assignment to Deltares, as part of the “Kennis voor Keringen”[1] program, to investigate the practical implications of the new approach for the work of Rijkswaterstaat.

Although the early debate had indicated that the key differences cannot be easily identified in general terms, the debate focussing on the governing equations was continued for a while, until it was decided to investigate the differences that result if various boundary conditions are calculated using reasonable material properties.

The cases that are considered, including the results that are obtained, are shortly described in Chapter 2. In Chapter 3 these results are discussed in general, including the practical implications. A conclusion and recommendation are given in Chapter 4.

[1] In English: Knowledge for (flood) defences.

2 Cases considered

2.1 Introduction

The investigation of the practical implications is focused on differences obtained with the well-established model by Biot and the new model by Van Damme & Den Ouden-Van der Horst. While Van Damme & Den Ouden-Van der Horst (2023) do no give a direct comparison between both models, in her master thesis Klein (2024) investigated both models and compared them. As part of the work reported here, Klein made additional comparisons, included to this report in the Annexes A and B. These comparisons are described and discussed in the following sections.

2.2 Thesis by Klein (2024)

For a theoretical problem, Klein defines various boundary conditions and applies these to both models. For the pore pressures, the numerical results are essentially the same. This is not surprising as basically the same equation is solved. The volumetric strains and the displacements, however, differ a lot in magnitude between both models. Moreover, in some comparable cases the displacements are in an opposite direction and spatial distribution also differs. However, Klein writes “note that the values for the volumetric strain and displacements are very small and could be considered as zero which is the steady state of Biot’s model.” (Klein, 2024:53).

A remark is made here regarding the optional assumption of incompressibility of water. This simplification is often made when applying Biot’s model, as well as in other fields of engineering like ‘fluid mechanics’ (cf. Van Damme & Den Ouden-Van der Horst, 2023:18). While Van Damme & Den Ouden-Van der Horst (2023) explore the implications of a truly incompressible fluid, i.e. $\beta = 0$, Klein sticks to physics and interprets ‘incompressible water’ as fully saturated water (Klein, 2024:22,25). Therefore, despite the title of her thesis, it only concerns cases of compressible pore water.

Klein also applied a one-dimensional expression of the new model to two cases for which experimental data is available. Details are given in Klein (2024), here only the graphs are repeated.

The first case concerns a vertical cylinder with a 1.8 m thick layer of (nearly) saturated sand covered by water, 0.2 m deep, with a cyclic water load on top. Both the density of the sand and the saturation degree have been varied in the experiments, as shown in Figure 2.1 and Figure 2.2, respectively.

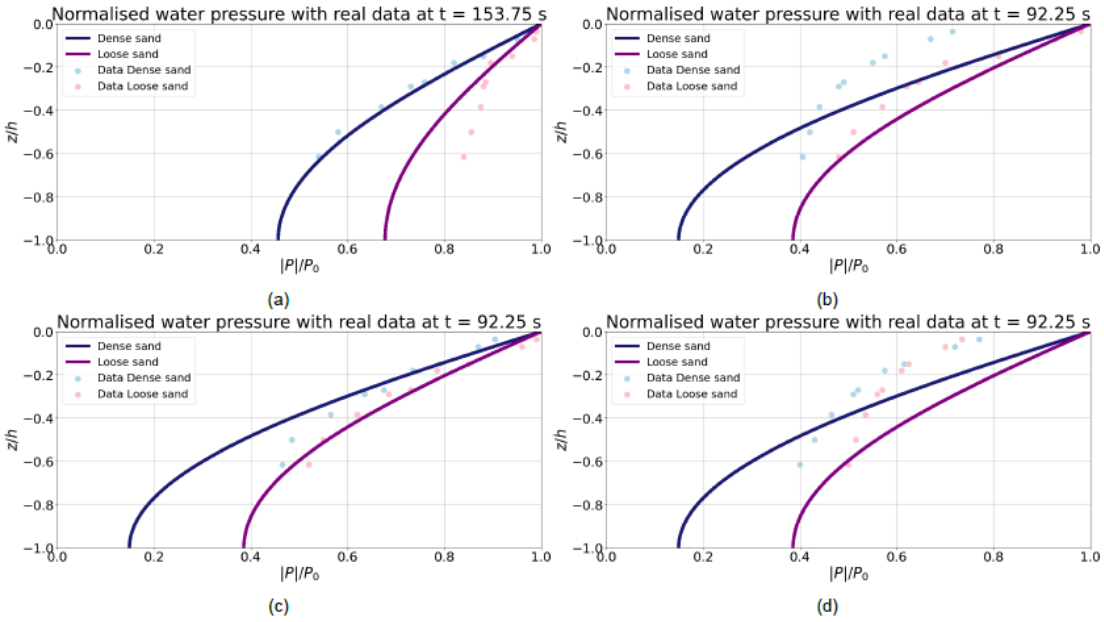

Figure 2.1 Figure 10.3 from Klein (2024), showing the influence of various densities according to the new model.

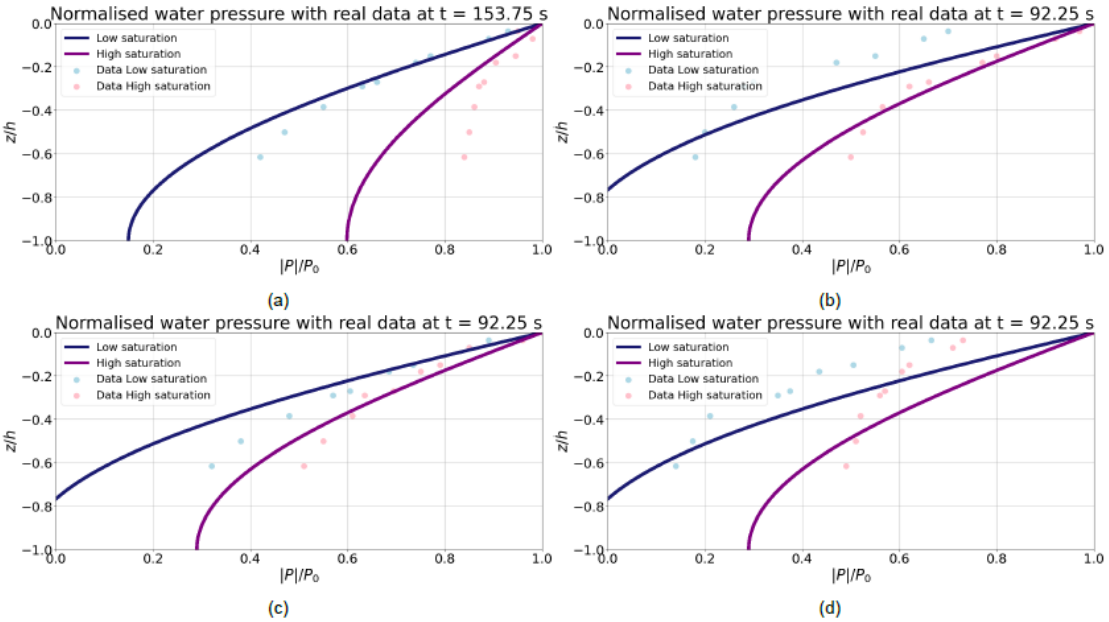

Figure 2.2 Figure 10.4 from Klein (2024), showing the influence of various degrees of saturation according to the new model.

The degree to which the new model agrees with the measurements varies. Sometimes, a close agreement is found (e.g. loose sand and t = 153.75 s), more often differences are found. Yet, for such problems the agreement is generally not bad, considering the difficulties to obtain reliable parameter values for material properties, assumed to be constant in the model. Note that for this case all material properties were assumed to be constant over depth. This is unlikely to be correct.

The second case concerns the pressures in a canal bed, generated by passing ships. Figure 2.3 shows water pressures for four passages.

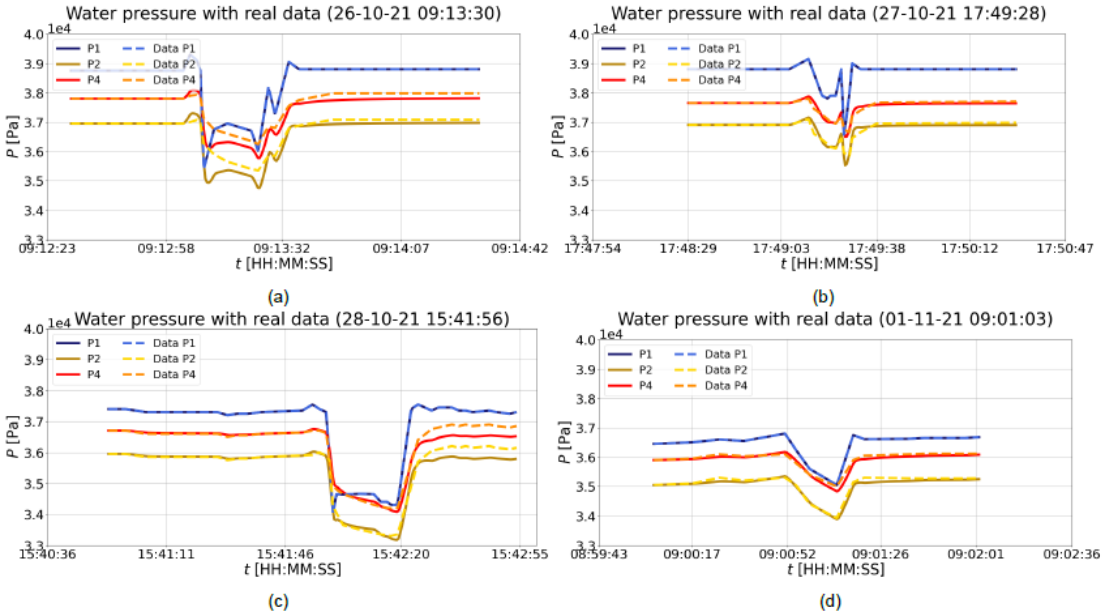

Figure 2.3 Figure 10.8 from Klein (2024), showing measured and calculated pressures at the bottom of a canal (P1), inside the sand-bentonite cover layer (P2) and below that layer in the sand (P3), during the passage of ships according to the new model.

For most situations, the calculations with the new model agree well with the measurements. The largest differences are found for the first case (Figure 2.3a), where especially the peaks in the response of the soil are not reproduced well. Yet, the peaks in the second case (Figure 2.3b) are followed closely.

These experimental results were not compared by Klein with Biot's model.

2.3 First addition by Klein (Annex A)

Upon a request from Deltares, Klein prepared an addition to her thesis, in which both models were compared for two additional cases. The report is included in Annex A.

For one of the cases, a 1D calculation was possible for both models. The resulting effective stress, volumetric strain, water pressure and displacement are shown in Figure 2.4. Their derivatives with respect to the distance are shown in Figure 2.5.

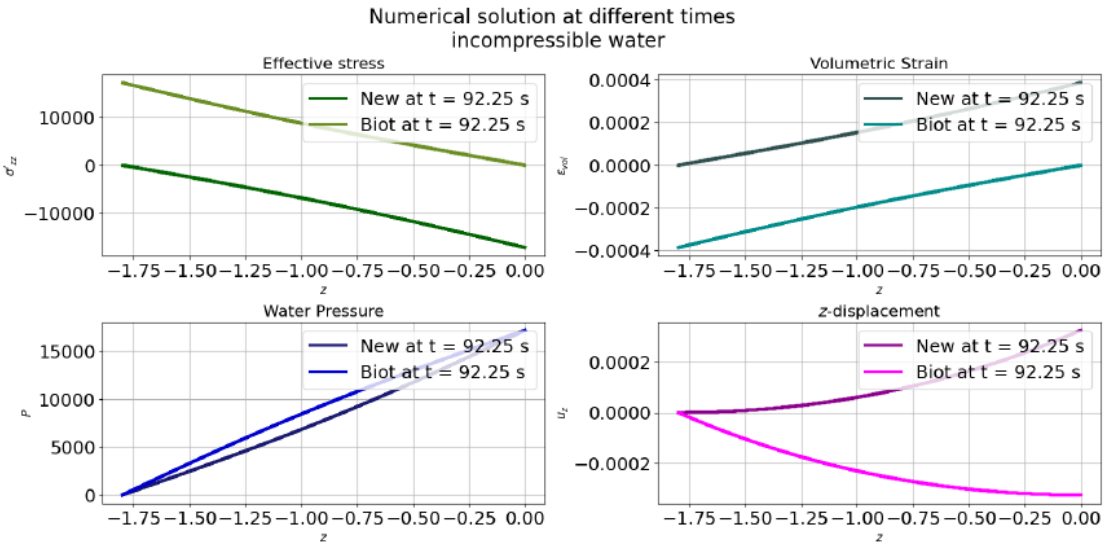

Figure 2.4 Figure 4.3 from Annex A, showing a comparison between both models for a 1D situation.

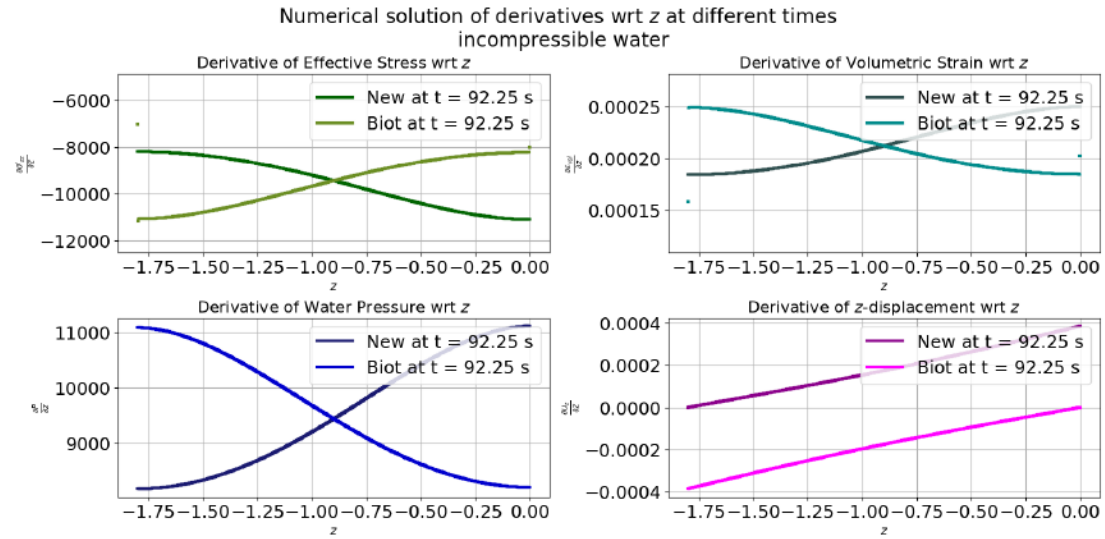

Figure 2.5 Figure 4.4 from Annex A, showing the derivatives of the previous figure with respect to the distance.

The most striking difference concerns the effective stresses. The new model follows the imposed boundary conditions, while for Biot's model the assumption regarding the effective stress being zero at the top, in accordance with Terzaghi's principle, leads to a hard reset at the top (z=0), as can be seen in the top left graph in Figure 2.4. This influences the strain and displacements too. Regarding the pore pressures, the difference is limited.

For the 2D calculations, both cases gave numerical results for both models. For the first case (section 5.1 in Annex A), results are largely similar for the pore pressure and the horizontal displacement. Yet, for the vertical displacement the values are larger for the new model and the spatial distribution is rather different compared to Biot's model. As a consequence, the volumetric strain of the new model is also larger, about a factor of two.

For the second case (section 5.2 in Annex A), the pore pressure and the horizontal displacement are comparable for both models. This also holds for the spatial distribution of the volumetric strain and the vertical displacement, yet here these two variables are about four times smaller for the new model than for Biot's model.

2.4 Second addition by Klein (Annex B)

Confusion about the meaning of the boundary conditions in the first report (Annex A) urged to make a second version, included in Annex B.

Here, no 1D solution is presented.

For both cases, the pore pressures are similar, as can be seen by comparing the lower left graph of Figure 3.1 with the corresponding graph in Figure 3.7 (case 1), and similarly for Figure 3.4 and Figure 3.10 (case 2).

For the volumetric strain and the horizontal and vertical displacements, the corresponding graphs look similar, yet regarding the extreme values.

- For case 1:
  - The volumetric strain is about three times larger with the new model than with Biot's model.
  - The horizontal displacement is also about three times larger with the new model than with Biot's model.
  - The vertical displacement is about three times smaller with the new model than with Biot's model.
- For case 2:
  - The volumetric strain is about three times larger with the new model than with Biot's model.
  - The horizontal displacement according to the new model is about two-third of the value obtained with Biot's model.
  - The vertical displacement is a bit more than two times smaller with the new model than with Biot's model.

In short, for both cases the deformations with the new model differ significantly from the deformations with Biot's model, although the pore pressures are similar.

3 Discussion

Both models give basically the same results for the pore pressures when the pore water is modelled as compressible. Small differences that occur in the numerical solutions are not significant and may be attributed to the numerical procedures that are applied. The implications of incompressible water ($\beta = 0$) have not been investigated by Klein (2024) and were also not investigated in this additional study.

Larger differences are found regarding the displacements and the related volumetric strain. These differences are up to a factor of three (both ways), while the spatial distribution is usually similar, but not always. For practical applications, a factor of three regarding displacements and volumetric strain is typically of significant importance. Reliable cases with measurements of deformations have not (yet) been calculated with both models.

It is clear that the models are different and produce different results regarding deformations. An question that easily pops up, is “Is the new model correct?”, as in: “Do the results by the model closely resemble reality?” However, this question can also be inverted: “Is Biot’s model correct?” For its primarily purpose, predicting the generation and dissipation of pore pressures, it is generally considered so, but in that regard both models perform equal. For deformations, sometimes good results are known with Biot’s model, while sometimes the accuracy is rather limited.

In this regard, an analogy with Bishop’s model for slope stability (Bishop, 1955) comes into mind. Although in this model severe simplifications are assumed – only momentum equilibrium is considered, no equilibrium of vertical forces and no equilibrium of horizontal forces – the model tends to give reasonably well results. Curious about this success, in spite of the simplifications made, Spencer investigated how this is possible, as described in a publication twelve years after Bishop’s, to which any curious reader is referred (Spencer, 1967). Similarly, Biot’s model could be quite correct, despite the simplifications that are made.

Considering the different ways in which Biot on the one side and Van Damme & Den Ouden-Van der Horst on the other side (and many years later!) derived their models, it can be speculated that the choices made by Biot resulted in a solution that gives a result that is roughly correct, not only with regard to the pore pressure but also with regard to the deformations, yet in some cases the solution may be more correct for the deformations than in other cases.

However, this does not necessarily mean that the new model is undoubtedly correct. It may be correct, while yet for instance the derivation of stiffness parameters from laboratory tests may need to be reconsidered. E.g., the derivation of the shear modulus from the measurements made during a triaxial test may be influenced by the governing approach, i.e. Biot’s model, so for the new model a different value may be derived from the same test results.

This will require additional research of a rather fundamental character, including e.g. a reconsideration of the interpretation of laboratory test results. This fits better at an academic level than at an applied research institute, and may take several years. Nevertheless, it is recommended that applied research institutes such as Deltares and TNO, to name a few Dutch examples, tap into that research to make it really applicable to practice, including the work of Rijkswaterstaat, as soon as possible.

4 Conclusion and recommendation

After considering several cases with the new model by Van Damme & Den Ouden-Van der Horst (2023), it can be concluded that it gives the same solution for the pore pressure field as Biot (1941) when considering compressible pore water, yet the deformation field may be different, up to a factor of (at least) three, with sometimes an overall different spatial distribution. Due to these differences it cannot be easily determined which of the two models generally resembles reality more closely.

On the basis of this study, it may be inferred that there may be a considerable impact on the accuracy of calculations in various civil engineering applications, where dynamic loads have an important effect. Moreover, yet outside the scope of this study, the new model may impact the practice of undrained analyses for basically transient situations, like stability analyses of embankments or failure analyses of dike revetments.

This would require a more widely scoped investigation, in which the implications of the approach by the new model can also be scrutinized, e.g. regarding the interpretation of laboratory and field tests.

It is therefore recommended that further (fundamental) research is carried out, initially at an academic level, and that results of this research are disseminated into practice as soon as possible, either directly or in cooperation with applied research institutes.

References

Biot (1941). M. Biot, General theory to three-dimensional consolidation, *Journal of Applied Physics* **62**:155-164.

Bishop (1955). Alan W. Bishop, The use of the slip circle in the analysis of slopes, *Géotechnique* **5**(1):7-17.

Klein (2024). F.P.M. Klein, *Compressible vs. incompressible pore water in fully-saturated poroelastic soil,* MSc thesis, TU Delft, Delft, 23 May 2024, https://diamhomes.ewi.tudelft.nl/~kvuik/numanal/klein_afst.pdf.

Spencer (1967). E. Spencer, A method of analysis of the stability of embankments assuming parallel inter-slice forces, *Géotechnique* **17**(1):11-26.

Van Damme & Den Ouden-Van der Horst (2023). M. van Damme & D. den Ouden-Van der Horst, An alternative process-based approach to predicting the response of water saturated porous media to hydrodynamic loads, *Journal of Porous Media* **27**(1):69-91, https://doi.org/10.1615/JPorMedia.2023045106.

A Two additional cases – October 17, 2024

Two additional cases on Msc thesis Compressible vs. incompressible water in poroelastic soil

Written for Deltares by ir. F.P.M. Klein

October 17, 2024

Contents

1

Introduction

This report is an extension on our Msc thesis last year [1]. In this report we will discribe two additional cases of boundary conditions for the model of Biot and the new model by Van Damme & Den Ouden-Van der Horst [2] for comparison between these two models in more detail.

In our literature report [3] and Msc thesis [1] we assumed that a positive pore water pressure is a pushing force and a negative pore water pressure is a pulling force. In Figure 1.1, the hydraulic load is denoted by the red arrows. Note that when the red arrow is pointing downwards there is a positive pressure on the soil (pushing force). On the other hand, when the red arrow is pointing upwards there is a negative pressure on the soil (pulling force) [1]. Furthermore, we have that the vorticity is zero everywhere on the domain.

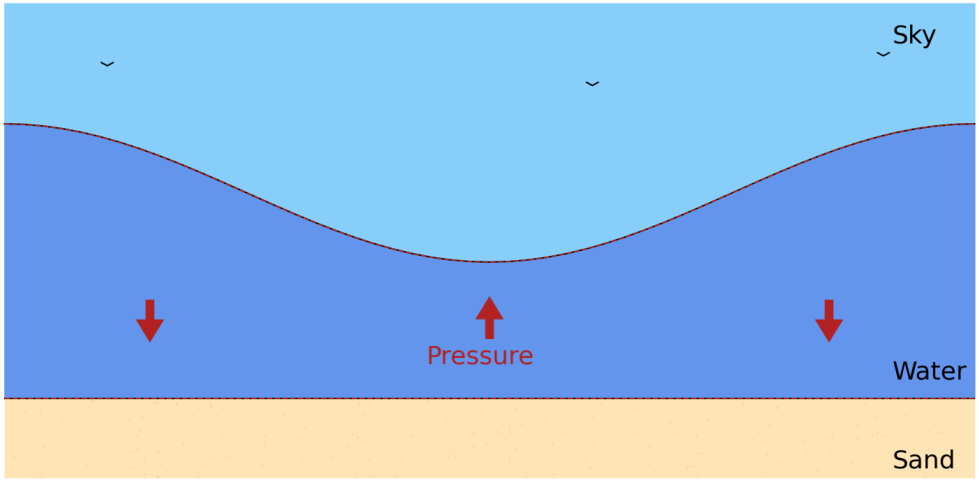

Figure 1.1: A flat foreshore subjected to water waves [1].

In Chapter 2 we will give a short recap of the two-dimensional governing equations for Biot's model in Section 2.1 and for the new model in Section 2.2. In Section 2.1.2 and in Section 2.2.2 we will introduce the two additional cases of boundary conditions for Biot's model and the new model in two dimensions, respectively. The first case is when the layer of soil is quicksand at the bottom. The second case is when the layer of soil is dry at the bottom. In Section 2.3 we will describe the initial conditions. In Section 2.1.3 and 2.2.3 we find the stationary solutions for Biot's model and the new model in one dimension, respectively. In Chapter 3 we will discuss the numerical models in one dimension and show the one-dimensional numerical results for Biot's model and the new model using the two different sets of boundary conditions. In Chapter 5 we will discuss the two-dimensional numerical results for Biot's model and the new model using the two different sets of boundary conditions. Finally, in Chapter 6 we will make some conclusions.

2

Models

In the next sections we will take a look into the two-dimensional governing equations of Biot's model and the new model of Van Damme & Den Ouden-Van der Horst. Note that we have vorticity $\omega := \frac{\partial u_x}{\partial z} - \frac{\partial u_z}{\partial x}$ is equal to zero [1]. Furthermore, we will determine the stationary solutions to Biot's model and the new model in one dimension.

2.1. Biot's model

In this section we will describe the governing equations of Biot's model and give the corresponding stationary model with its solution.

2.1.1. Governing equations (2D)

It is common to describe Biot's model by three governing equations in two dimensions which are given by the conservation of mass equation and the momentum balance equation [1]. The conservation of mass equation in one dimension is given by

$$\frac{\gamma_w}{K_s} p\beta \frac{\partial P}{\partial t} - \nabla^2 P + \frac{\gamma_w}{K_s} \frac{\partial}{\partial t}\left(\frac{\partial u_x}{\partial x} + \frac{\partial u_z}{\partial z}\right) = 0. \tag{2.1}$$

Respectively, the horizontal and vertical momentum balance equations are given by

$$-(\lambda + 2\mu)\nabla^2 u_x + \frac{\partial P}{\partial x} = 0, \tag{2.2}$$

$$-(\lambda + 2\mu)\nabla^2 u_z + \frac{\partial P}{\partial z} = 0. \tag{2.3}$$

To determine the volumetric strain we use the following equation

$$\epsilon = \frac{\partial u_z}{\partial z}. \tag{2.4}$$

2.1.2. Boundary conditions (2D)

In this section we will discuss two sets of boundary conditions for the two-dimensional model of Biot. Both sets differ one boundary condition at the bottom $z = -n_z$. Most of the boundary conditions are from our Msc thesis [1].

In Biot's model it is common to set the total normal stress equal to the hydrodynamic load and to suppose that the normal effective stress equals zero which results in the water pressure being equal to the hydrodynamic load [3]. Then we set the one-dimensional boundary conditions $\sigma'_{zz} := -(\lambda + 2\mu)\frac{\partial u_z}{\partial z} = 0$ and $P = F_{zz}(t)$ at $z = 0$, where $F_{zz}(t)$ represents the normal stress and only depends on time and is chosen to be positive [1]. The shear stress is set equal to zero.

At the bottom, $z = -n_z$, we assume that for case I the normal effective stress at the bottom equals zero and for case II the pore water pressure equals zero, i.e. $\sigma'_{zz} = 0$ for case I or $P = 0$ for case II. Similarly, at $x = 0$ and $x = -n_x$ we get that $\frac{\partial u_z}{\partial x} = 0$, $\frac{\partial u_x}{\partial z} = 0$, $u_x = 0$, $\frac{\partial \epsilon_{\text{vol}}}{\partial x} = 0$ and $\frac{\partial P}{\partial x} = 0$ [1].

Then we get that for Biot's model the sets of boundary conditions are given by

B-I

$$\text{for } z=0: \begin{cases} -\mu\left(\frac{\partial u_x}{\partial z}+\frac{\partial u_z}{\partial x}\right)=F_{xz} \\ P=F_{zz} \\ -\lambda\frac{\partial u_x}{\partial x}-(\lambda+2\mu)\frac{\partial u_z}{\partial z}=0 \end{cases}, \tag{2.5}$$

$$\text{for } z=-n_z: \begin{cases} \frac{\partial u_x}{\partial z}=\frac{\partial P}{\partial z}=0 \\ -\lambda\frac{\partial u_x}{\partial x}-(\lambda+2\mu)\frac{\partial u_z}{\partial z}=0 \end{cases}, \tag{2.6}$$

$$\text{and for } x=0 \text{ and } x=n_x: \begin{cases} u_x=\frac{\partial u_z}{\partial x}=\frac{\partial P}{\partial x}=0 \end{cases}, \tag{2.7}$$

$$\text{for } z=0: \begin{cases} -\mu\left(\frac{\partial u_x}{\partial z}+\frac{\partial u_z}{\partial x}\right)=F_{xz} \\ P=F_{zz} \\ -\lambda\frac{\partial u_x}{\partial x}-(\lambda+2\mu)\frac{\partial u_z}{\partial z}=0 \end{cases}, \tag{2.8}$$

$$\text{for } z=-n_z: \begin{cases} u_z=\frac{\partial u_x}{\partial z}=0 \\ P=0 \end{cases}, \tag{2.9}$$

$$\text{and for } x=0 \text{ and } x=n_x: \begin{cases} u_x=\frac{\partial u_z}{\partial x}=\frac{\partial P}{\partial x}=0 \end{cases}, \tag{2.10}$$

We choose that [1]

$$F_{zz}(t)=0.5\gamma_w H\sin\left(2\pi\frac{t}{T}\right), \tag{2.11}$$

where γ_w [N/m^3] the specific weight of the pore water, H [m] is the wave height and T [s] the wave period.

Note that when the normal effective stress at the bottom is zero at the bottom, there is no normal stress acting on the soil particles and the total normal stress will only depend on the pore water pressure. For example, this could happen when there is a layer of quicksand at the bottom of the computational domain. On the other hand, when the the pore water pressure at the bottom is zero, then there is no normal stress acting on the pore water particles and the total normal stress will only depend on the normal effective stress. This could eventually happen if there is a layer of dry soil at the bottom of the computational domain.

2.1.3. Stationary model (1D)

When we assume that $t\Longrightarrow\infty$, we find the stationary model of Biot's model in one dimension. Note that for $t\Longrightarrow\infty$ we have that $F_{zz}(t)$ becomes constant in time, say F, and $\frac{\partial}{\partial t}=0$. Then the stationary model of Biot is given by

$$\begin{cases} \frac{\partial^2 P}{\partial z^2}=0, \\ -(\lambda+2\mu)\frac{\partial^2 u_z}{\partial z^2}+\frac{\partial P}{\partial z}=0, \end{cases} \tag{2.12}$$

and $\epsilon=\frac{\partial u_z}{\partial z}$. Solving Equation (2.12) we get the following solutions

$$\begin{cases} P(z)=c_1 z+c_2, \\ u_z(z)=\frac{c_1}{2(\lambda+2\mu)}z^2+c_3 z+c_4, \end{cases} \tag{2.13}$$

(I) When using the boundary conditions from set B-I we get that $c_1=c_3=0$, $c_2=F$ and $c_4\in\mathbb{R}$. Then Equation (2.13) becomes

$$\begin{cases} P(z)=F, \\ u_z(z)=c_4. \end{cases} \tag{2.14}$$

Then we also get that

$$\epsilon(z)=0. \tag{2.15}$$

Note that we thus have infinitely many solutions for u_z. Constant c_4 can only be determine if we also set u_z equal to a certain constant at a boundary. However, this additional boundary condition can not be implemented, since there already are boundary conditions for u_z at both boundaries.

(II) When using the boundary conditions from set B-II we get that $c_1 = \frac{F}{n_z}$, $c_2 = F$, $c_3 = 0$ $c_4 = -\frac{Fn_z}{2(\lambda+2\mu)}$. Then Equation (2.13) becomes

$$\begin{cases} P(z) = \frac{F}{n_z} z + F, \\ u_z(z) = \frac{F}{2n_z(\lambda+2\mu)} z^2 - \frac{Fn_z}{2(\lambda+2\mu)}. \end{cases} \tag{2.16}$$

Then we also get that

$$\epsilon(z) = \frac{F}{n_z(\lambda+2\mu)} z. \tag{2.17}$$

2.2. New model

In this section we will describe the governing equations of Biot's model in two dimensions and give the one-dimensional stationary model with its solution.

2.2.1. Governing equations (2D)

In two dimensions the model of Van Damme & Den Ouden-Van der Horst can be described by four governing equations, namely the equation for the pore water pressure (conservation of mass), the equation for the volumetric strain and the equation for displacement [2]. The derivation of these equations can be found in our master thesis [1]. The equation for the water pressure is given by

$$\frac{\gamma_w}{K_s} p\beta \frac{\partial P}{\partial t} - \nabla^2 P + \frac{\gamma_w}{K_s} \frac{\partial \epsilon_{\text{vol}}}{\partial t} = 0. \tag{2.18}$$

The equation for the volumetric strain is given by

$$\frac{\gamma_w}{K_s} p\beta \frac{\partial P}{\partial t} - \nabla^2 \epsilon_{\text{vol}} + \frac{\gamma_w}{K_s} \frac{\partial \epsilon_{\text{vol}}}{\partial t} = 0. \tag{2.19}$$

The equation for the displacement in horizontal and vertical direction is given by

$$\frac{\partial^2 u_x}{\partial x^2} = \frac{\partial \epsilon_{\text{vol}}}{\partial x}, \tag{2.20}$$

$$\frac{\partial^2 u_z}{\partial z^2} = \frac{\partial \epsilon_{\text{vol}}}{\partial z}. \tag{2.21}$$

2.2.2. Boundary conditions (2D)

In this section we will discuss two sets of boundary conditions used for the new model in two dimensions. Both sets differ one boundary condition at the bottom $z = -n_z$. Most of the boundary conditions are from our Msc thesis [1].

In the new model we assume, like in Biot's model, that the pore water pressure equals the hydrodynamic load and that the shear stress is zero. However, we do not set the normal effective stress equal to zero [1]. In stead, the vertical momentum balance equation can be used again which is in one dimension given by $-(\lambda+2\mu)\frac{\partial \epsilon_{\text{vol}}}{\partial z} + \frac{P}{\partial z} = 0$ [2].

Then the sets of boundary conditions for the new model are given by [1]

N-I

$$\text{for } z = 0: \begin{cases} -\mu\left(\frac{\partial u_x}{\partial z} + \frac{\partial u_z}{\partial x}\right) = F_{xz} \\ P = F_{zz} \\ -(\lambda+2\mu)\frac{\partial \epsilon_{\text{vol}}}{\partial z} + \frac{\partial P}{\partial z} = 0 \end{cases}, \tag{2.22}$$

$$\text{for } z = -n_z: \begin{cases} \frac{\partial u_x}{\partial z} = \frac{\partial P}{\partial z} = \frac{\partial \epsilon_{\text{vol}}}{\partial z} = 0 \\ -\lambda\frac{\partial u_z}{\partial z} - 2\mu\epsilon_{\text{vol}} = 0 \end{cases}, \tag{2.23}$$

$$\text{and for } x = 0 \text{ and } x = n_x: \begin{cases} u_x = \frac{\partial u_z}{\partial x} = \frac{\partial P}{\partial x} = \frac{\partial \epsilon_{\text{vol}}}{\partial x} = 0 \end{cases}, \tag{2.24}$$

$$\text{for } z=0: \begin{cases} -\mu\left(\frac{\partial u_x}{\partial z}+\frac{\partial u_z}{\partial x}\right)=F_{xz} \\ P=F_{zz} \\ -(\lambda+2\mu)\frac{\partial \epsilon_{\text{vol}}}{\partial z}+\frac{\partial P}{\partial z}=0 \end{cases}, \tag{2.25}$$

$$\text{for } z=-n_z: \begin{cases} u_z=\frac{\partial u_x}{\partial z}=0 \\ P=0 \end{cases}, \tag{2.26}$$

$$\text{and for } x=0 \text{ and } x=n_x: \left\{ u_x=\frac{\partial u_z}{\partial x}=\frac{\partial P}{\partial x}=\frac{\partial \epsilon_{\text{vol}}}{\partial x}=0 \right. , \tag{2.27}$$

Note that $-\lambda\frac{\partial u_z}{\partial z}-2\mu\epsilon_{\text{vol}}=0 \Longleftrightarrow -\lambda\frac{\partial u_x}{\partial x}-(\lambda+2\mu)\frac{\partial u_z}{\partial z}=0$, since $\epsilon_{\text{vol}}=\frac{\partial u_x}{\partial x}+\frac{\partial u_z}{\partial z}$.

2.2.3. Stationary model (1D)

When assuming that $t \Longrightarrow \infty$, we find the stationary model for the new model in one dimension. Then the stationary model of Van Damme & Den Ouden-Van der Horst is given by

$$\begin{cases} \frac{\partial^2 P}{\partial z^2}=0, \\ \frac{\partial^2 \epsilon_{\text{vol}}}{\partial z^2}=0, \\ \frac{\partial^2 u_z}{\partial z^2}=\frac{\partial \epsilon_{\text{vol}}}{\partial z}. \end{cases} \tag{2.28}$$

After solving Equation (2.28) we get the following solutions

$$\begin{cases} P(z)=c_1 z+c_2, \\ \epsilon_{\text{vol}}(z)=c_3 z+c_4, \\ u_z(z)=\frac{c_3}{2}z^2+c_5 z+c_6. \end{cases} \tag{2.29}$$

(I) When using the boundary conditions from set N-I we get that $c_1=\frac{F}{n_z}$, $c_2=F$, $c_3=\frac{F}{n_z(\lambda+2\mu)}$, $c_4=c_5=\frac{F}{(\lambda+2\mu)}$ and $c_6 \in \mathbb{R}$. Note that we can now impose an extra boundary conditions for u_z, since we have an extra governing equations. When we set $u_z=0$, we get $c_6=\frac{Fn_z}{2(\lambda+2\mu)}$. Then Equation (2.29) becomes

$$\begin{cases} P(z)=\frac{F}{n_z}z+F, \\ \epsilon_{\text{vol}}(z)=\frac{F}{n_z(\lambda+2\mu)}z+\frac{F}{\lambda+2\mu}, \\ u_z(z)=\frac{F}{2n_z(\lambda+2\mu)}z^2+\frac{F}{\lambda+2\mu}z+\frac{Fn_z}{2(\lambda+2\mu)}. \end{cases} \tag{2.30}$$

(II) When using the boundary conditions from set N-II we get that $c_1=\frac{F}{n_z}$, $c_2=F$, $c_3=\frac{F}{n_z(\lambda+2\mu)}$, $c_4=c_5=\frac{F}{(\lambda+2\mu)}$ and $c_6=\frac{Fn_z}{2(\lambda+2\mu)}$. Then Equation (2.29) becomes

$$\begin{cases} P(z)=\frac{F}{n_z}z+F, \\ \epsilon_{\text{vol}}(z)=\frac{F}{n_z(\lambda+2\mu)}z+\frac{F}{\lambda+2\mu}, \\ u_z(z)=\frac{F}{2n_z(\lambda+2\mu)}z^2+\frac{F}{\lambda+2\mu}z+\frac{Fn_z}{2(\lambda+2\mu)}. \end{cases} \tag{2.31}$$

Note that the solutions to the new model are the same for both set of boundary conditions N-I and N-II. This is caused by the vertical momentum balance equation which holds everywhere in combination with the boundary condition $-(\lambda+2\mu)\epsilon_{\text{vol}}+P=0$ at the surface $z=0$.

2.3. Initial conditions

We assume that at the start, $t=0$, everything is at rest [3]. Therefore, no stresses act on the surface in the beginning which means that there are no stresses and displacements at time $t=0$ [2]. According to [1], this means that the volumetric strain and pressure must be zero too. Then we have that

$$u_z|_{t=0}=\epsilon_{\text{vol}}|_{t=0}=P|_{t=0}=0.$$

3

Numerical models (1D)

3.1. Biot's model

For Biot's model the Finite-Element Method is used for discretisation in space and the Euler method for discretisation in time. After applying the discretisation first in space and second in time, the final numerical model can be derived. These steps in between can be read in our literature report [3] or Msc thesis [1].

3.1.1. Boundary conditions case I

Using the boundary condition set B-I given in Section 2.1.2, we get the following numerical equations after applying the Finite-Element Method described in our literature report [3].

$$\begin{cases} \frac{\gamma_w}{K_s} C\bar{\boldsymbol{u}}^z_t + \frac{\gamma_w}{K_s} p\beta A\bar{\boldsymbol{P}}_t + (B+SC)\bar{\boldsymbol{P}} & = \boldsymbol{0} \\ (\lambda+2\mu)B\bar{\boldsymbol{u}}^z + C\bar{\boldsymbol{P}} & = \boldsymbol{0}, \quad , \\ A\bar{\boldsymbol{\epsilon}} & = C\bar{\boldsymbol{u}}^z. \end{cases} \tag{3.1}$$

where $A_{i,j} = \int_{-n_z}^{0} N_i N_j \mathrm{d}z, B_{i,j} = \int_{-n_z}^{0} \frac{\partial N_i}{\partial z}\frac{\partial N_j}{\partial z}\mathrm{d}z, C_{i,j} = \int_{-n_z}^{0} N_i \frac{\partial N_j}{\partial z}\mathrm{d}z$ and $SC_{i,j} = N_i(-n_z)\frac{\partial N_j(-n_z)}{\partial z}$. We can write Equation (3.1) as one systems of matrix-vector multiplication

$$M^t \boldsymbol{S}_t + M\boldsymbol{S} = \boldsymbol{f}, \tag{3.2}$$

where

$$M^t = \begin{bmatrix} \frac{\gamma_w}{K_s} p\beta A & \frac{\gamma_w}{K_s} C & \emptyset \\ \emptyset & \emptyset & \emptyset \\ \emptyset & \emptyset & \emptyset \end{bmatrix}, \quad M = \begin{bmatrix} B+SC & \emptyset & \emptyset \\ C & (\lambda+2\mu)B & \emptyset \\ \emptyset & -C & A \end{bmatrix}, \quad \boldsymbol{S} = \begin{bmatrix} \bar{\boldsymbol{P}} \\ \bar{\boldsymbol{u}}^z \\ \bar{\boldsymbol{\epsilon}} \end{bmatrix}, \quad \boldsymbol{S}_t = \begin{bmatrix} \frac{\partial \bar{\boldsymbol{P}}}{\partial t} \\ \frac{\partial \bar{\boldsymbol{u}}^z}{\partial t} \\ \frac{\partial \bar{\boldsymbol{\epsilon}}}{\partial t} \end{bmatrix}, \quad \boldsymbol{f}(t) = \begin{bmatrix} \boldsymbol{F}(t) \\ \boldsymbol{0} \\ \boldsymbol{0}, \end{bmatrix} \tag{3.3}$$

where $\boldsymbol{F}_n = F_z z(t)$ and $\boldsymbol{F}_i = 0$ for $i \in [0, n-1]$ for n elements. Note that the Neumann boundary conditions are included. The Dirichlet boundary conditions will be included after time discretisation. We will apply the Backward-Euler method for time discretisation. When assuming that matrix $\left(M^t + \Delta t M\right)$ is invertible, we get that for $k \geq 0$

$$\boldsymbol{S}^{k+1} = M^{-1}_{\text{new}}\left(M_{\text{old}}\boldsymbol{S}^k + \Delta t \boldsymbol{f}^{k+1}\right), \tag{3.4}$$

where $M_{\text{new}} = M^t + \Delta t M$ and $M_{\text{old}} = M^t$, k represents a step in time and $k+1$ the next step in time. The Dirichlet boundary conditions can be included by setting the corresponding rows of matrices M_{new} and M_{old} to zero and then putting pivots in these same rows of M_{new}. However, since we now have two boundary conditions for the vertical displacement, namely a Neumann and a Dirichlet boundary condition at $z = -n_z$, one boundary condition will override the other. Therefore, we can not solve this numerical model of Biot using set boundary conditions B-I.

3.1.2. Boundary conditions case II

Using the boundary condition set B-II given in Section 2.1.2, we get the following numerical equations after applying the Finite-Element Method described in our literature report [3].

$$\begin{cases} \frac{\gamma_w}{K_s} C\bar{\boldsymbol{u}}_t^z + \frac{\gamma_w}{K_s} p\beta A\bar{\boldsymbol{P}}_t + B\bar{\boldsymbol{P}} & = \boldsymbol{0} \\ (\lambda+2\mu)B\bar{\boldsymbol{u}}^z + C\bar{\boldsymbol{P}} & = \boldsymbol{0}, \\ A\bar{\boldsymbol{\epsilon}} & = C\bar{\boldsymbol{u}}^z. \end{cases}, \tag{3.5}$$

where $A_{i,j} = \int_{-n_z}^{0} N_i N_j \mathrm{d}z, B_{i,j} = \int_{-n_z}^{0} \frac{\partial N_i}{\partial z}\frac{\partial N_j}{\partial z}\mathrm{d}z$ and $C_{i,j} = \int_{-n_z}^{0} N_i \frac{\partial N_j}{\partial z}\mathrm{d}z$. We can write Equation (3.5) as two systems of matrix-vector multiplication

$$\begin{cases} M^t \boldsymbol{S}_t + M\boldsymbol{S} & = \boldsymbol{f} \\ A\bar{\boldsymbol{\epsilon}} & = C\bar{\boldsymbol{u}}^z \end{cases}, \tag{3.6}$$

where

$$M^t = \begin{bmatrix} \frac{\gamma_w}{K_s} p\beta A & \frac{\gamma_w}{K_s} C \\ \emptyset & \emptyset \end{bmatrix}, \quad M = \begin{bmatrix} B & \emptyset \\ C & (\lambda+2\mu)B \end{bmatrix}, \quad \boldsymbol{S} = \begin{bmatrix} \bar{\boldsymbol{P}} \\ \bar{\boldsymbol{u}}^z \end{bmatrix}, \quad \boldsymbol{S}_t = \begin{bmatrix} \frac{\partial \bar{\boldsymbol{P}}}{\partial t} \\ \frac{\partial \bar{\boldsymbol{u}}^z}{\partial t} \end{bmatrix}, \quad \boldsymbol{f}(t) = \begin{bmatrix} \boldsymbol{F}(t) \\ \boldsymbol{0} \end{bmatrix}. \tag{3.7}$$

Note that the Neumann boundary conditions are included. The Dirichlet boundary conditions will be included after time discretisation. We will apply the Backward-Euler method for time discretisation. When assuming that matrices $\left(M^t + \Delta t M\right)$ and A are invertible, we get that

$$\begin{cases} \boldsymbol{S}^{k+1} & = M_{\text{new}}^{-1}\left(M_{\text{old}}\boldsymbol{S}^k + \Delta t \boldsymbol{f}^{k+1}\right) \\ \bar{\boldsymbol{\epsilon}}^{k+1} & = A^{-1} C \bar{\boldsymbol{u}_{\boldsymbol{z}}}^{k+1} \end{cases}, \tag{3.8}$$

where $M_{\text{new}} = M^t + \Delta t M$ and $M_{\text{old}} = M^t$.

3.2. New model

For the new model, we also use the Finite-Element Method for discretisation in space and the Euler method for discretisation in time. After applying the discretisation first in space and second in time, the final numerical model can be derived. These steps in between can be read in our literature report [3] or Msc thesis [1].

3.2.1. Boundary conditions case I

Using the boundary condition set N-I given in Section 2.1.2, we get the following numerical equations after applying the Finite-Element Method described in our literature report [3] are given by

$$\begin{cases} \frac{\gamma_w}{K_s} A\bar{\boldsymbol{\epsilon}}_t + \frac{\gamma_w}{K_s} p\beta A\bar{\boldsymbol{P}}_t + B\bar{\boldsymbol{P}} + (\lambda+2\mu)SC\bar{\boldsymbol{\epsilon}} & = \boldsymbol{0} \\ \frac{\gamma_w}{K_s} A\bar{\boldsymbol{\epsilon}}_t + \frac{\gamma_w}{K_s} p\beta A\bar{\boldsymbol{P}}_t + (\lambda+2\mu)B\bar{\boldsymbol{\epsilon}} & = \boldsymbol{0}, \\ C\bar{\boldsymbol{u}}^z & = A\bar{\boldsymbol{\epsilon}}. \end{cases}, \tag{3.9}$$

where $A_{i,j} = \int_{-n_z}^{0} N_i N_j \mathrm{d}z, B_{i,j} = \int_{-n_z}^{0} \frac{\partial N_i}{\partial z}\frac{\partial N_j}{\partial z}\mathrm{d}z$ and $C_{i,j} = \int_{-n_z}^{0} N_i \frac{\partial N_j}{\partial z}\mathrm{d}z$. We can write Equation (3.9) as two systems of matrix-vector multiplication

$$\begin{cases} M^t \boldsymbol{S}_t + M\boldsymbol{S} & = \boldsymbol{f} \\ C\bar{\boldsymbol{u}}^z & = A\bar{\boldsymbol{\epsilon}} \end{cases}, \tag{3.10}$$

where

$$M^t = \begin{bmatrix} \frac{\gamma_w}{K_s} p\beta A & \frac{\gamma_w}{K_s} A \\ \frac{\gamma_w}{K_s} p\beta A & \frac{\gamma_w}{K_s} A \end{bmatrix}, \quad M = \begin{bmatrix} B+SC & \emptyset \\ \emptyset & (\lambda+2\mu)B \end{bmatrix}, \quad \boldsymbol{S} = \begin{bmatrix} \bar{\boldsymbol{P}} \\ \bar{\boldsymbol{\epsilon}} \end{bmatrix}, \quad \boldsymbol{S}_t = \begin{bmatrix} \frac{\partial \bar{\boldsymbol{P}}}{\partial t} \\ \frac{\partial \bar{\boldsymbol{\epsilon}}}{\partial t} \end{bmatrix}, \quad \boldsymbol{f}(t) = \begin{bmatrix} \boldsymbol{F}(t) \\ \boldsymbol{0} \end{bmatrix}. \tag{3.11}$$

Note that the Neumann boundary conditions are included. The Dirichlet boundary conditions will be included after time discretisation. We will apply the Backward-Euler method for time discretisation. When assuming that matrices $\left(M^t + \Delta t M\right)$ and C are invertible, we get that

$$\begin{cases} \boldsymbol{S}^{k+1} & = M_{\text{new}}^{-1}\left(M_{\text{old}}\boldsymbol{S}^k + \Delta t \boldsymbol{f}^{k+1}\right) \\ \bar{\boldsymbol{u}_{\boldsymbol{z}}}^{k+1} & = C^{-1} A \bar{\boldsymbol{\epsilon}}^{k+1} \end{cases}, \tag{3.12}$$

where $M_{\text{new}} = M^t + \Delta t M$ and $M_{\text{old}} = M^t$.

3.2.2. Boundary conditions case II

Using the boundary condition set N-I given in Section 2.1.2, we get the following numerical equations after applying the Finite-Element Method described in our literature report [3] are given by

$$\begin{cases} \frac{\gamma_w}{K_s} A\bar{\boldsymbol{\epsilon}}_t + \frac{\gamma_w}{K_s} p\beta A\bar{\boldsymbol{P}}_t + B\bar{\boldsymbol{P}} & = \boldsymbol{0} \\ \frac{\gamma_w}{K_s} A\bar{\boldsymbol{\epsilon}}_t + \frac{\gamma_w}{K_s} p\beta A\bar{\boldsymbol{P}}_t + (\lambda+2\mu)B\bar{\boldsymbol{\epsilon}} + SC\bar{\boldsymbol{P}} & = \boldsymbol{0}, \quad , \\ C\bar{\boldsymbol{u}}^z & = A\bar{\boldsymbol{\epsilon}}. \end{cases} \tag{3.13}$$

where $A_{i,j} = \int_{-n_z}^{0} N_i N_j \mathrm{d}z, B_{i,j} = \int_{-n_z}^{0} \frac{\partial N_i}{\partial z} \frac{\partial N_j}{\partial z} \mathrm{d}z$ and $C_{i,j} = \int_{-n_z}^{0} N_i \frac{\partial N_j}{\partial z} \mathrm{d}z$. We can write Equation (3.13) as two systems of matrix-vector multiplication

$$\begin{cases} M^t \boldsymbol{S}_t + M\boldsymbol{S} & = \boldsymbol{f} \\ C\bar{\boldsymbol{u}}^z & = A\bar{\boldsymbol{\epsilon}} \end{cases}, \tag{3.14}$$

where

$$M^t = \begin{bmatrix} \frac{\gamma_w}{K_s} p\beta A & \frac{\gamma_w}{K_s} A \\ \frac{\gamma_w}{K_s} p\beta A & \frac{\gamma_w}{K_s} A \end{bmatrix}, \quad M = \begin{bmatrix} B & \emptyset \\ \emptyset & (\lambda+2\mu)(B+SC) \end{bmatrix}, \quad \boldsymbol{S} = \begin{bmatrix} \bar{\boldsymbol{P}} \\ \bar{\boldsymbol{\epsilon}} \end{bmatrix}, \quad \boldsymbol{S}_t = \begin{bmatrix} \frac{\partial \bar{\boldsymbol{P}}}{\partial t} \\ \frac{\partial \bar{\boldsymbol{\epsilon}}}{\partial t} \end{bmatrix}, \quad \boldsymbol{f}(t) = \begin{bmatrix} \boldsymbol{F}(t) \\ \boldsymbol{0} \end{bmatrix}. \tag{3.15}$$

Note that the Neumann boundary conditions are included. The Dirichlet boundary conditions will be included after time discretisation. We will apply the Backward-Euler method for time discretisation. When assuming that matrices $\left(M^t + \Delta t M\right)$ and C are invertible, we get that

$$\begin{cases} \boldsymbol{S}^{k+1} & = M_{\text{new}}^{-1}\left(M_{\text{old}}\boldsymbol{S}^k + \Delta t \boldsymbol{f}^{k+1}\right) \\ \bar{\boldsymbol{u}}_{\boldsymbol{z}}{}^{k+1} & = C^{-1} A\bar{\boldsymbol{\epsilon}}^{k+1} \end{cases}, \tag{3.16}$$

where $M_{\text{new}} = M^t + \Delta t M$ and $M_{\text{old}} = M^t$.

4

Numerical results (1D)

In this section we will discuss the numerical solutions found for the numerical models assuming incompressible pore water and using sets boundary conditions B-I and (BII) for Biot's model and N-I and N-II for the new model. For the first set of boundary conditions (Case I) we will only present the numerical solutions for the normal effective stress, the volumetric strain, pore water pressure and the vertical displacement to the new numerical model in Section 4.1, since we can not solve the numerical model of Biot uniquely as described in Section 3.1.1. For the second set of boundary conditions (Case II) we will present the numerical solutions for the normal effective stress, volumetric strain, pore water pressure and vertical displacement to Biot's model and the numerical solutions for these variables to the new model in one plot. This will be denoted in Section 4.2. For both cases, we will also show the derivatives of these variables.

The values of the parameters are given by Table 4.1, 4.2 and 4.3.

Table 4.1: Parameters of one layer of sandy deposit [4].

Soil properties	**Symbols**	**Values**
Hydraulic conductivity [m/s]	K_s	$1.8 \cdot 10^{-4}$
Porosity	p	0.425
Poisson ratio	υ_p	0.3
Shear modulus [Pa]	μ	$1.27 \cdot 10^{7}$
Specific weight of water [N/m^3]	γ_w	9810

Table 4.2: Parameters of compressibility equation given by $\beta = s\beta_0 + \frac{1-s}{P_0}$.

Soil properties	**Symbols**	**Values**
Degree of saturation [4]	s	1.0
Compressibility of pure water [5]	β_0	$0.5 \cdot 10^{-9}$
Absolute pressure in the water [Pa] [5]	P_0	10^5

Table 4.3: Parameters of the waves [4].

Wave properties	**Symbols**	**Values**
Wave period [s]	T	9
Wave height [m]	H	3.5

4.1. Boundary conditions case I

When using the set of boundary conditions given by N-I for the new numerical model, the solutions for the normal effective stress σ'_{zz}, the volumetric strain ϵ_{vol}, pore water pressure P and the vertical displacement u_z to the new numerical model are shown in Figure 4.1. The x-axis represents the depth z going from $-n_z$ to 0, where $n_z = 1.8$ metres is chosen. The y-axis represents the variable. The units of the variables are given in the caption of the figure.

Then we find that the solutions are approximately linear functions for the normal effective stress, the volumetric strain and the water pressure and the solution for the vertical displacement is a bit parabolic. We expect such solutions over time according to the stationary solutions given by Equation (2.30). In Figure 4.1 we find the relation $(\lambda + 2\mu)\epsilon_{\text{vol}} = P$ and in Figure 4.2 we find the relation $(\lambda + 2\mu)\frac{\partial \epsilon_{\text{vol}}}{\partial z} = \frac{\partial P}{\partial z}$. In Figure 4.1 and Figure 4.2 we also find that indeed the relation $\epsilon_{\text{vol}} = \frac{\partial u_z}{\partial z}$ holds. Furthermore, we find that the boundary conditions given by N-I hold.

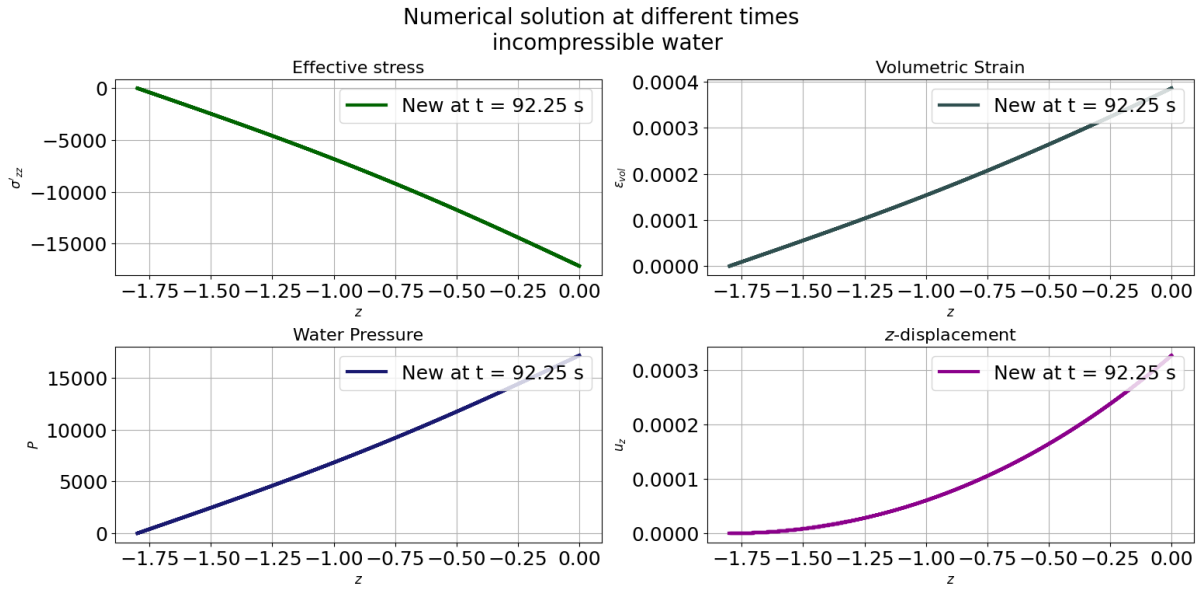

Figure 4.1: σ'_{zz} [Pa], ϵ_{vol} [-], P [Pa], u_z [m] at $t = 92.25$s, when water is assumed to be incompressible ($\beta = 5 \cdot 10^{-10}$) and the set of boundary conditions used is N-I.

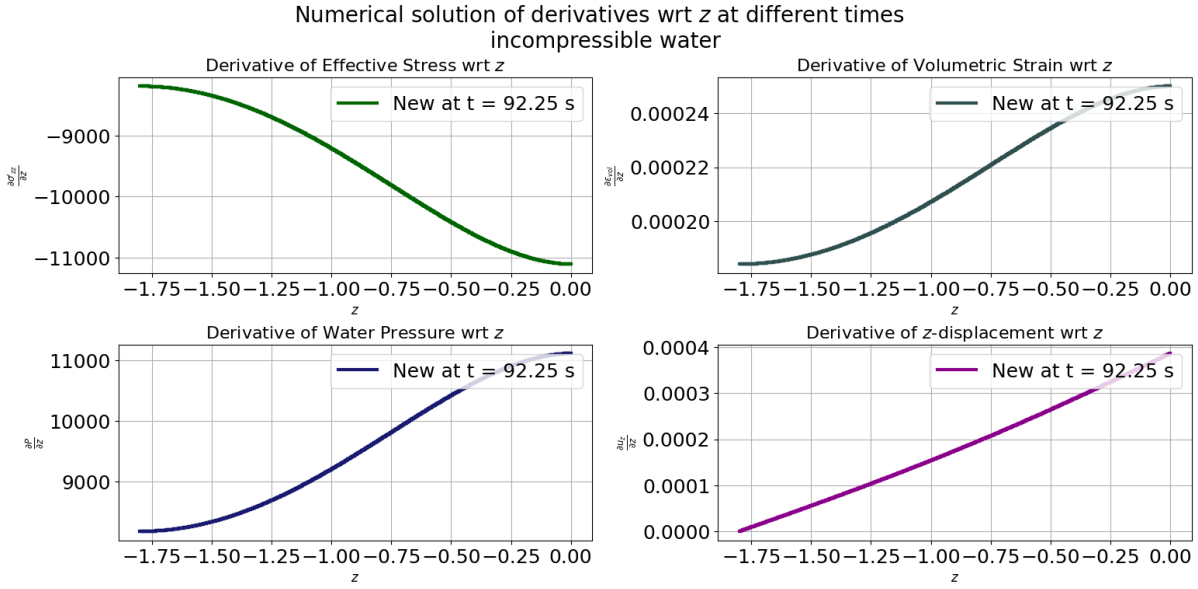

Figure 4.2: Derivatives of $\sigma'_{zz}, \epsilon_{\text{vol}}, P, u_z$ at $t = 92.25$s with respect to z, when water is assumed to be incompressible ($\beta = 5 \cdot 10^{-10}$) and the set of boundary conditions used is N-I.

4.2. Boundary conditions case II

When using the set of boundary conditions given by B-II for Biot's numerical model and N-II for the new numerical model, the solutions for the normal effective stress σ'_{zz}, the volumetric strain ϵ_{vol}, pore water pressure P and the vertical displacement u_z to Biot's numerical model and the new numerical model are shown in Figure 4.3. The x-axis represents the depth z going from $-n_z$ to 0, where $n_z = 1.8$ metres is chosen. The y-axis represents the variable. The units of the variables are given in the caption of the figure.

Then we find again that the solutions to the new model are approximately linear functions for the normal effective stress, the volumetric strain and the water pressure and the solution for the vertical displacement is a bit parabolic which is expected because of the stationary solutions given by Equation (2.31). We find similar behaviour for the solutions to the numerical model of Biot. The solutions for the pore water pressure to both models converge to the same stationary solution. In Figure 4.3 we find the relation $(\lambda+2\mu)\epsilon_{\text{vol}} = P$ for the new model and $(\lambda+2\mu)\epsilon_{\text{vol}} = P - F_{zz}$. In Figure 4.4 we find the relation $(\lambda+2\mu)\frac{\partial \epsilon_{\text{vol}}}{\partial z} = \frac{\partial P}{\partial z}$ for both Biot's model and the new model. In Figure 4.3 and Figure 4.4 we also find that indeed the relation $\epsilon_{\text{vol}} = \frac{\partial u_z}{\partial z}$ holds. Furthermore, we find that the boundary conditions given by B-II hold for Biot's model and N-II for the new model.

Note that the solutions for the normal effective stress and volumetric strain differ by a constant in space, approximately. Note that the solutions for the normal effective stress, volumetric strain and vertical displacements for Biot's model and the new model differ in sign. This results in a vertical displacement of the soil in opposite directions for both models. Since we have a one-dimensional setting, we have that the volumetric strain equals the derivative of the vertical displacement with respect to z. Since we set $u_z = 0$ at $z = -n_z$, we get a negative vertical displacement when the water pressure is positive and a negative volumetric strain. This is the case for the one-dimensional Biot's model. However, when the water pressure is positive and the volumetric strain positive, we get a positive vertical displacement. This is the case for the one-dimensional new model. Typically, we expect the vertical displacement to be negative [1], when the pore water pressure is positive (compression). In our literature report [3], we also found that this latter did not hold for the new model in one dimension. This could be done due to the fact that the simplifications made for the one dimension. In Chapter 5 we will present the solutions for both cases in two dimensions.

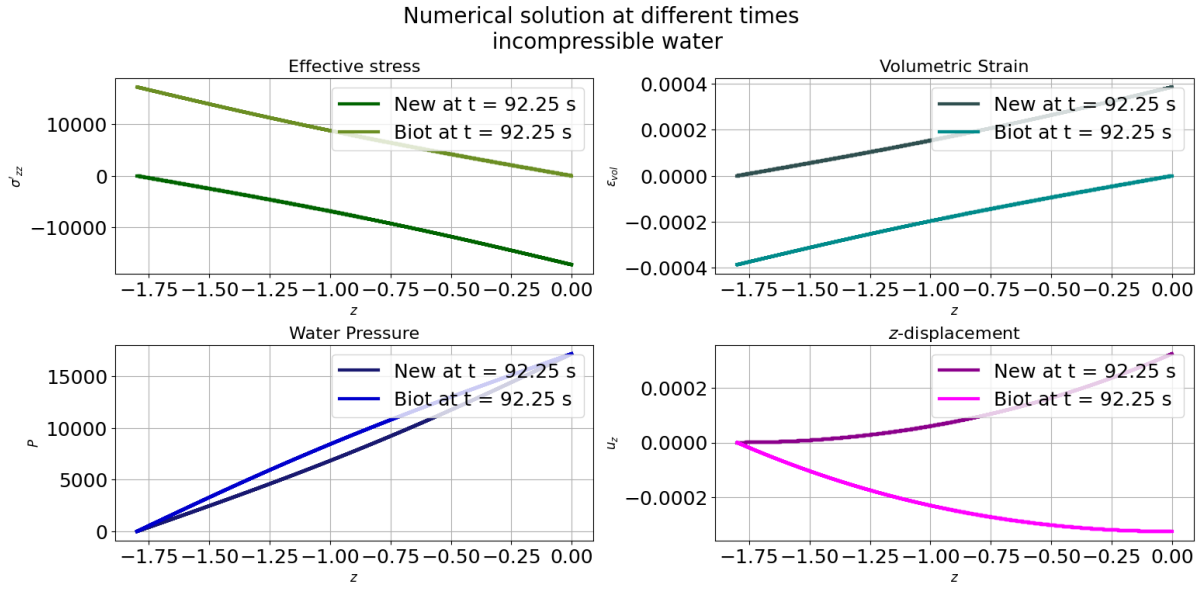

Figure 4.3: σ'_{zz} [Pa], ϵ_{vol} [-], P [Pa], u_z [m] at $t = 92.25$s, when water is assumed to be incompressible ($\beta = 5 \cdot 10^{-10}$) and the set of boundary conditions used is B-II for Biot's numerical model and N-II for the new numerical model.

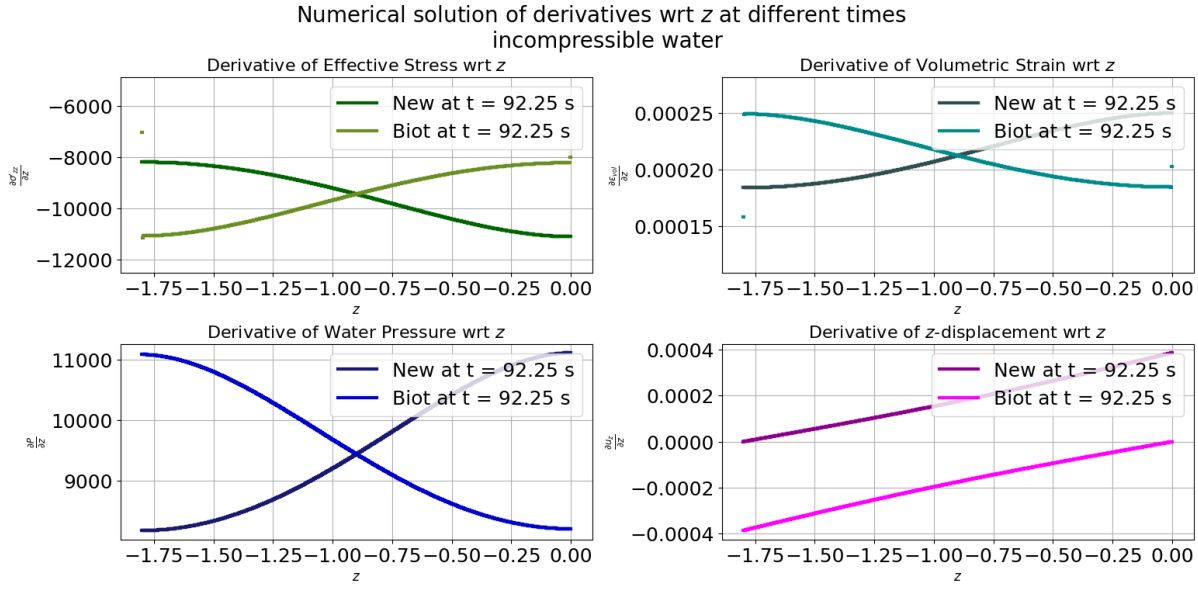

Figure 4.4: Derivatives of $\sigma'_{zz}, \epsilon_{\text{vol}}, P, u_z$ at $t = 92.25$s with respect to z, when water is assumed to be incompressible ($\beta = 5 \cdot 10^{-10}$) and the set of boundary conditions used is B-II for Biot's numerical model and N-II for the new numerical model.

5

Numerical results (2D)

We will now look into the numerical results in two dimensions in order to be able to compare the models better. For the numerical model in two dimensions we use the same methods as for 1D. So we apply the Finite-Element Method to the models for discretisation in space and the Backward-Euler method for discretisation in time. The steps taken are described in our Msc thesis [1] in Chapter 4 and Section 5.1.1 for Biot's model, and Chapter 7 and Section 8.1.1 for the new model. We choose $n_z = -2$ and $n_x = 1$ which means that the computational domain becomes $[0,1] \times [-2,0]$. We also set the hydraulic load in two dimensions to be [1]

$$F_{zz}(x,t) = 0.5\gamma_w H \sin\left(2\pi \frac{t}{T}\right) \cos\left(2\pi \frac{x}{L}\right), \tag{5.1}$$

where γ_w [N/m^3] the specific weight of the pore water, H [m] is the wave height, L [m] the length of the wave, T [s] the wave period.

The values of the parameters are given by Table 4.1, 4.2 and 4.3. Furthermore, we set the wave length L [m] equal to n_x.

5.1. Boundary conditions case I

Using boundary conditions B-I for Biot's model, we find the results shown in Figures 5.1, 5.2 and 5.3. When using boundary conditions N-I for the new model, we find the results shown in Figures 5.4, 5.5 and 5.6. Then we find that the differences between the solutions water pressure and horizontal displacement are similar for both models. The volumetric strain behaves the same for Biot's model and the new model, but it is about two times smaller for Biot's model than for the new model. The momentum balance equations hold for the new model but not for Biot's model. However, we find that the vertical displacement of the new model behaves differently and has values much smaller than for Biot's model. Typically, we expect the soil particles to move downwards when the pore water pressure is positive. However, in quicksand the soil particles are emerged by water. Therefore, when there is positive pore water pressure and no normal effective stress at point $x = x^*$, there is a bit of soil particles going downwards at point $x = x^*$ and then sideways upwards movement of soil particles at the points next to $x = x^*$.

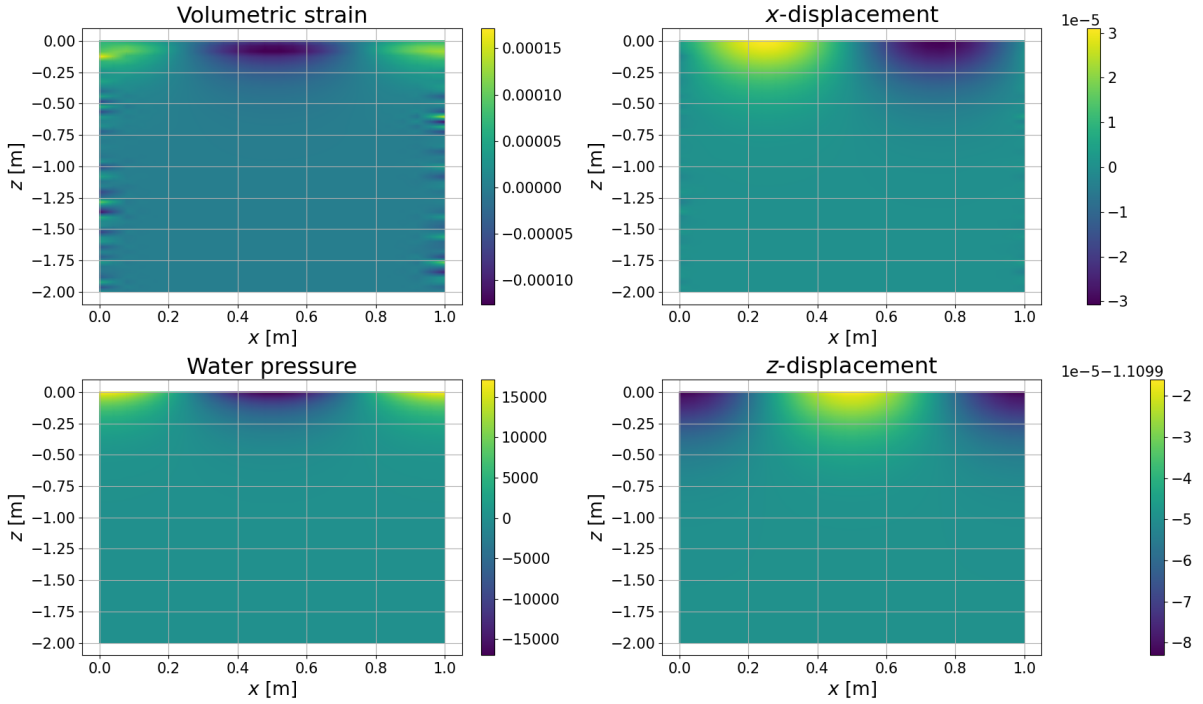

Figure 5.1: ϵ_{vol} [-], P [Pa], u_x [m] and u_z [m] at $t = 92.25$s, when water is assumed to be incompressible ($\beta = 5 \cdot 10^{-10}$) and the set of boundary conditions used is B-I.

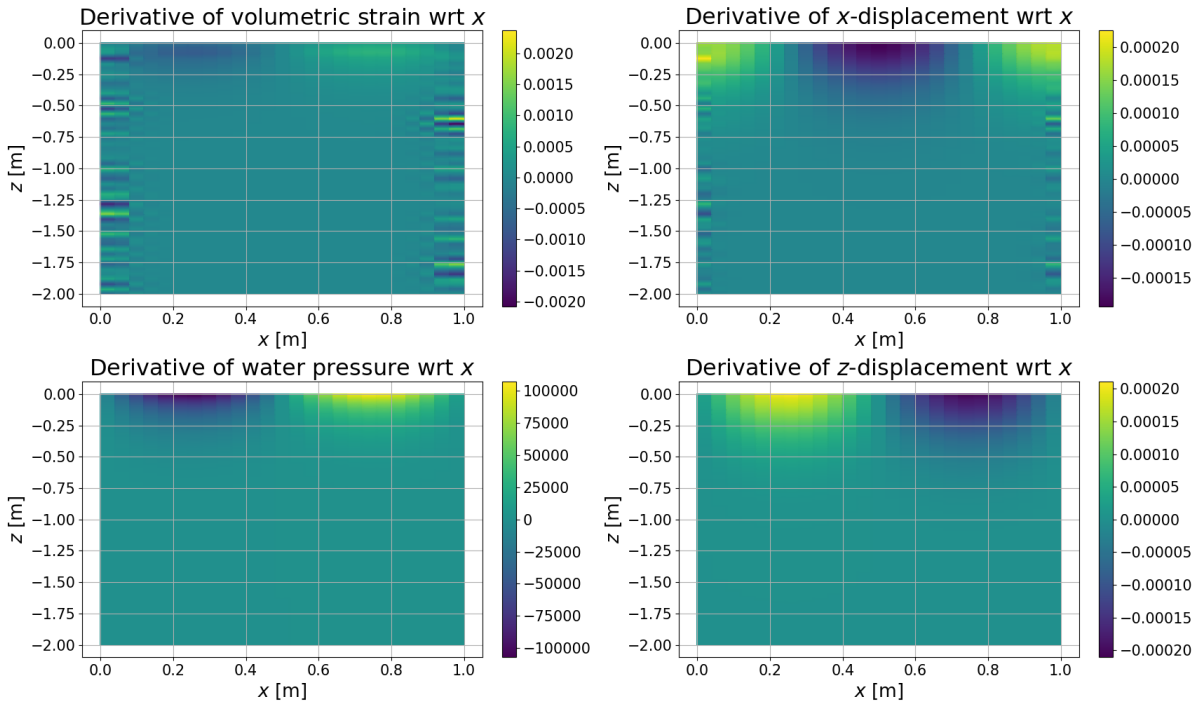

Figure 5.2: Derivatives of $\epsilon_{\text{vol}}, P, u_x, u_z$ at $t = 92.25$s with respect to x, when water is assumed to be incompressible ($\beta = 5 \cdot 10^{-10}$) and the set of boundary conditions used is B-I.

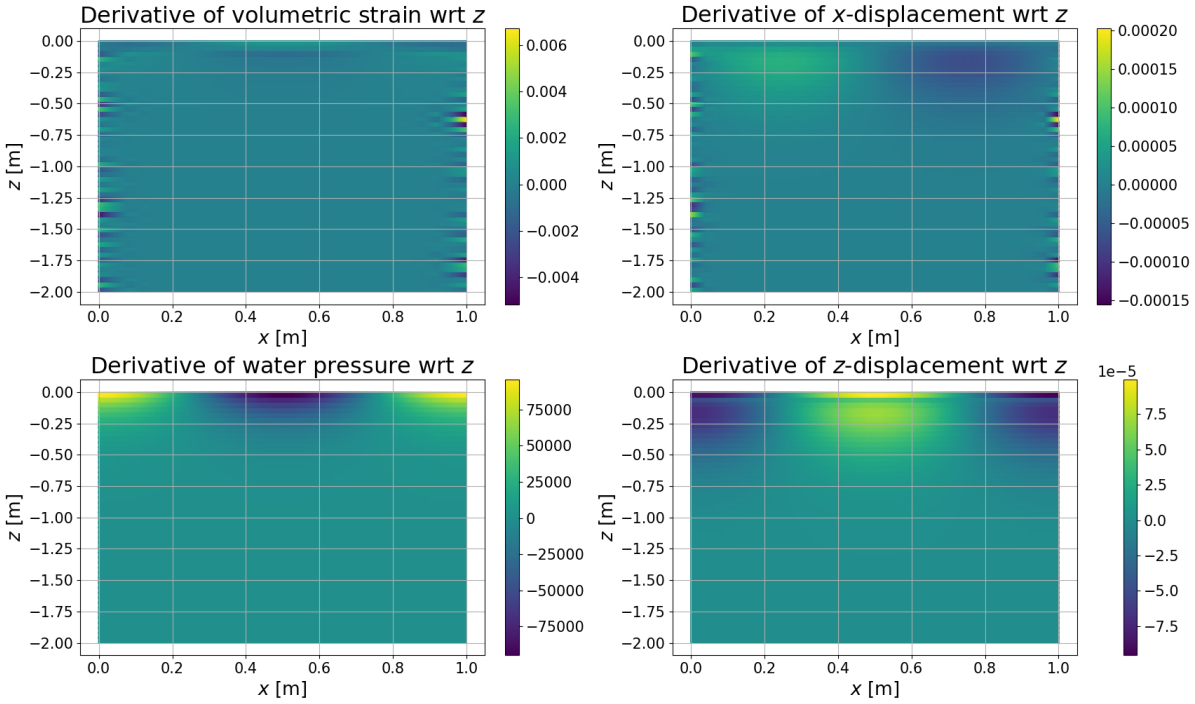

Figure 5.3: Derivatives of $\sigma'_{zz}, \epsilon_{\text{vol}}, P, u_x, u_z$ at $t = 92.25$s with respect to z, when water is assumed to be incompressible ($\beta = 5 \cdot 10^{-10}$) and the set of boundary conditions used is B-I.

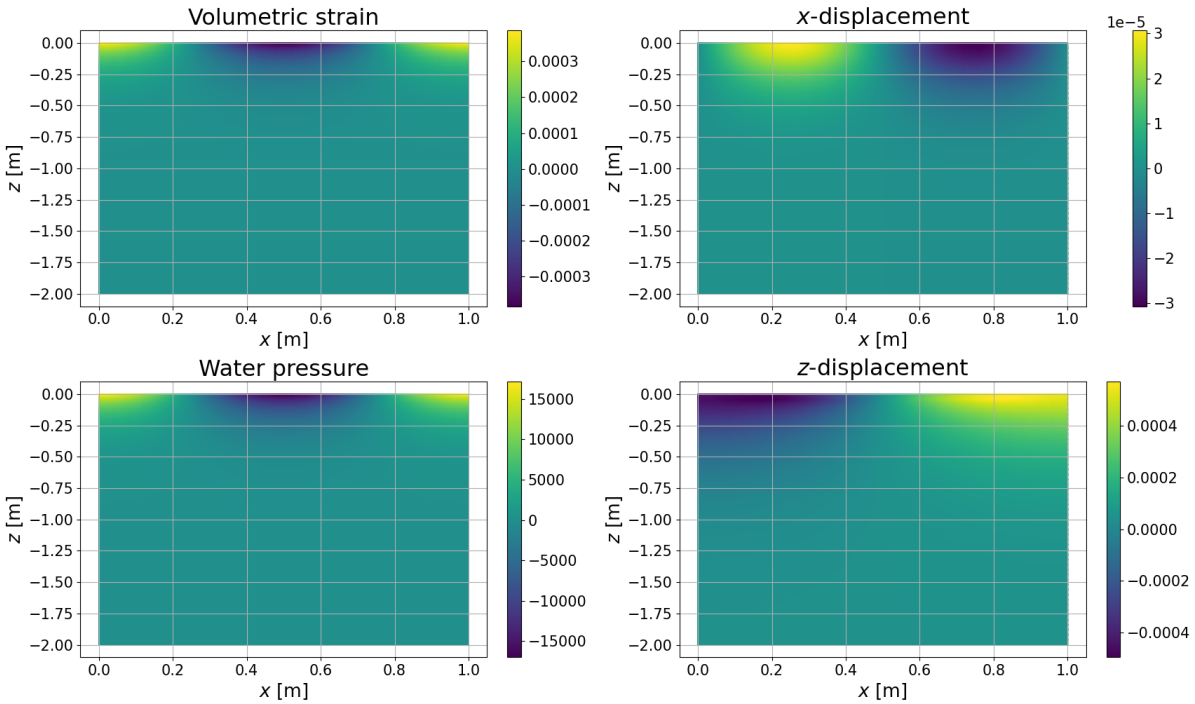

Figure 5.4: ϵ_{vol} [-], P [Pa], u_x [m] and u_z [m] at $t = 92.25$s, when water is assumed to be incompressible ($\beta = 5 \cdot 10^{-10}$) and the set of boundary conditions used is N-I.

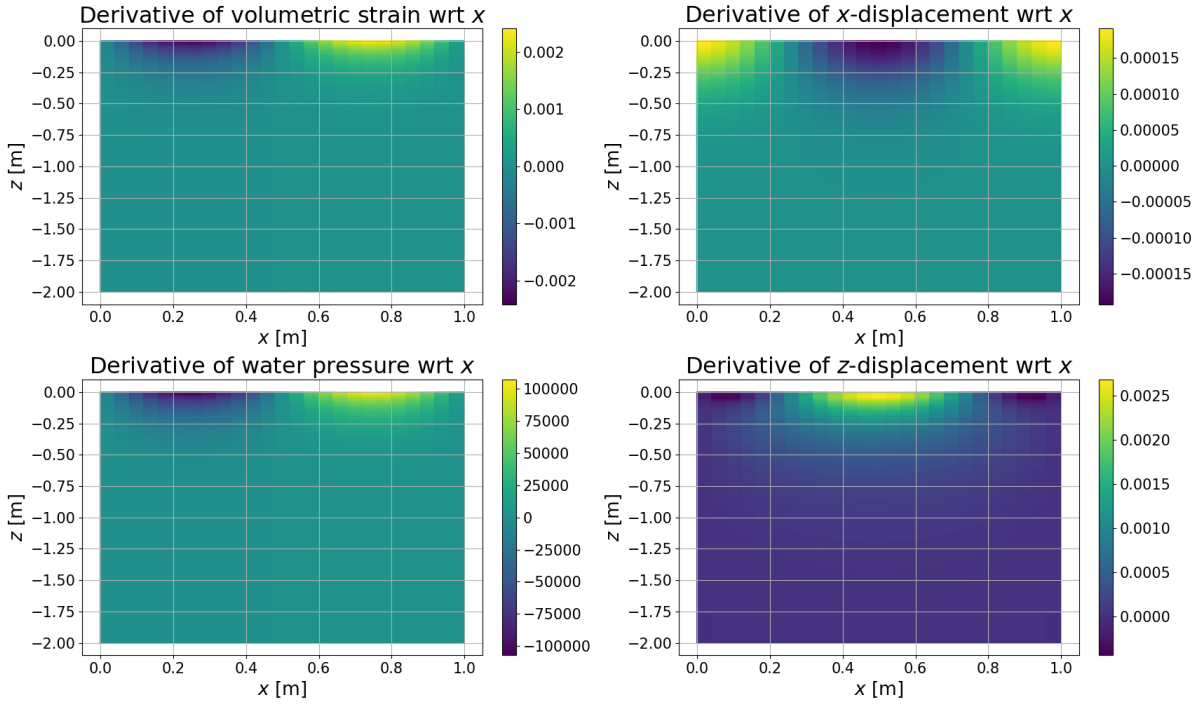

Figure 5.5: Derivatives of $\epsilon_{\text{vol}}, P, u_x, u_z$ at $t = 92.25$s with respect to x, when water is assumed to be incompressible ($\beta = 5 \cdot 10^{-10}$) and the set of boundary conditions used is N-I.

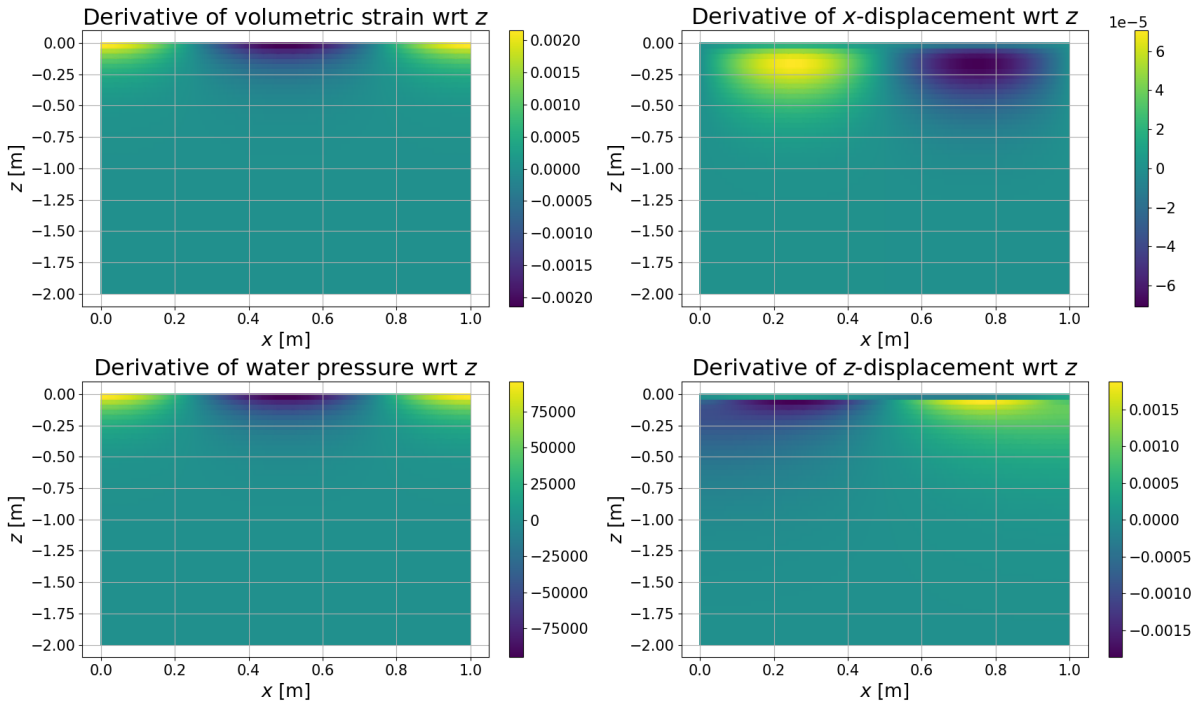

Figure 5.6: Derivatives of $\sigma'_{zz}, \epsilon_{\text{vol}}, P, u_x, u_z$ at $t = 92.25$s with respect to z, when water is assumed to be incompressible ($\beta = 5 \cdot 10^{-10}$) and the set of boundary conditions used is N-I.

5.2. Boundary conditions case II

Using boundary conditions B-II for Biot's model, we find the results shown in Figures 5.7, 5.8 and 5.9. When using boundary conditions N-II for the new model, we find the results shown in Figures 5.10, 5.11 and 5.12. Then we find that the differences between the solutions for the water pressure and horizontal displacement are similar for both models. The solution for the volumetric strain behaves similar for both models the but is about four times smaller for Biot's model than for the new model. The solution for the vertical displacement behaves also similar for both models but is about four times larger for Biot's model than for the new model.

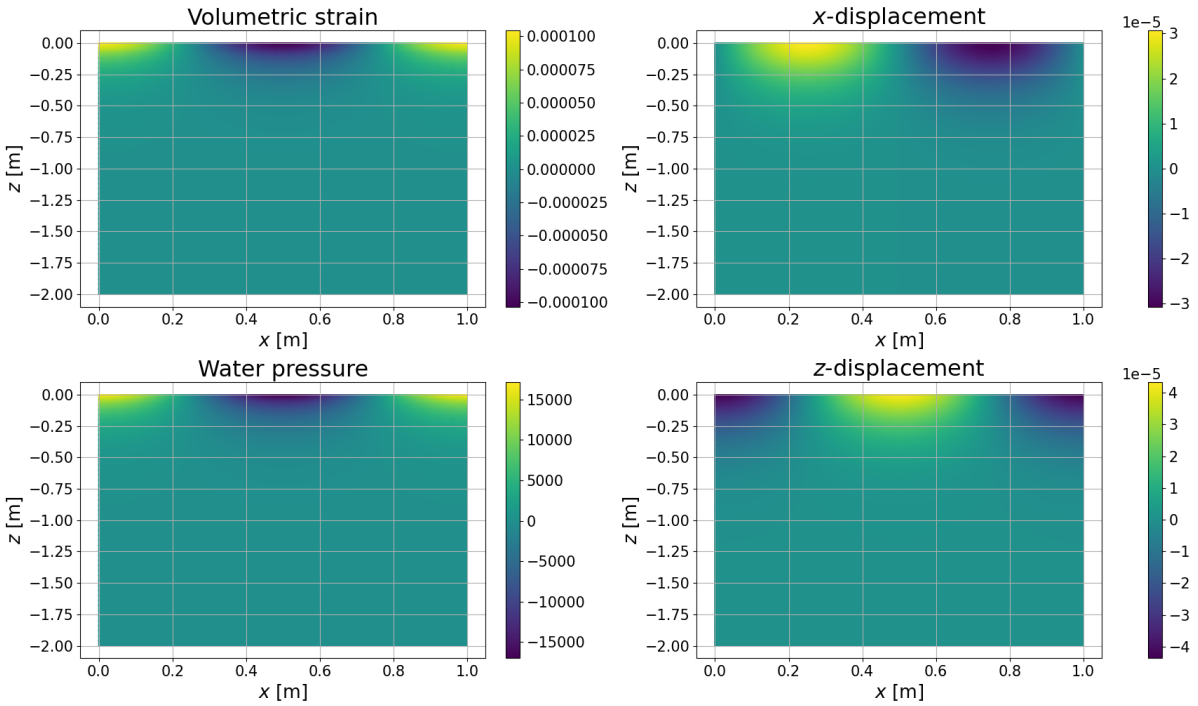

Figure 5.7: ϵ_{vol} [-], P [Pa], u_x [m] and u_z [m] at $t = 92.25$s, when water is assumed to be incompressible ($\beta = 5 \cdot 10^{-10}$) and the set of boundary conditions used is B-II.

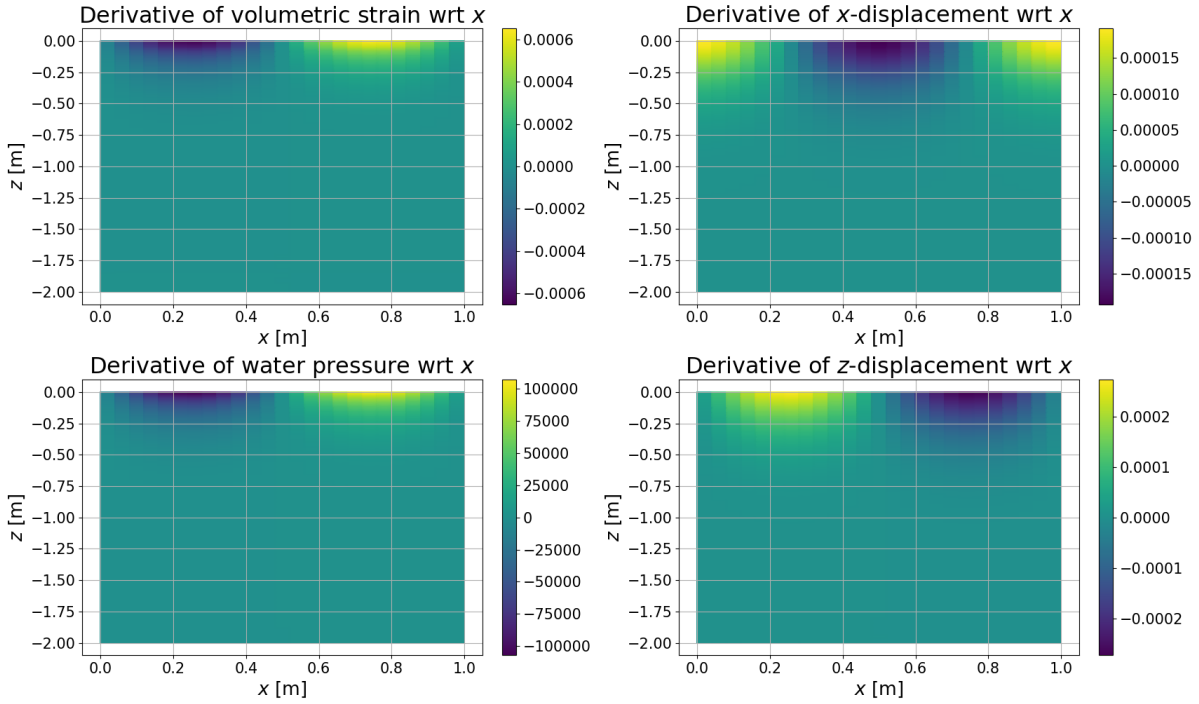

Figure 5.8: Derivatives of $\epsilon_{\text{vol}}, P, u_x, u_z$ at $t = 92.25$s with respect to x, when water is assumed to be incompressible ($\beta = 5 \cdot 10^{-10}$) and the set of boundary conditions used is B-II.

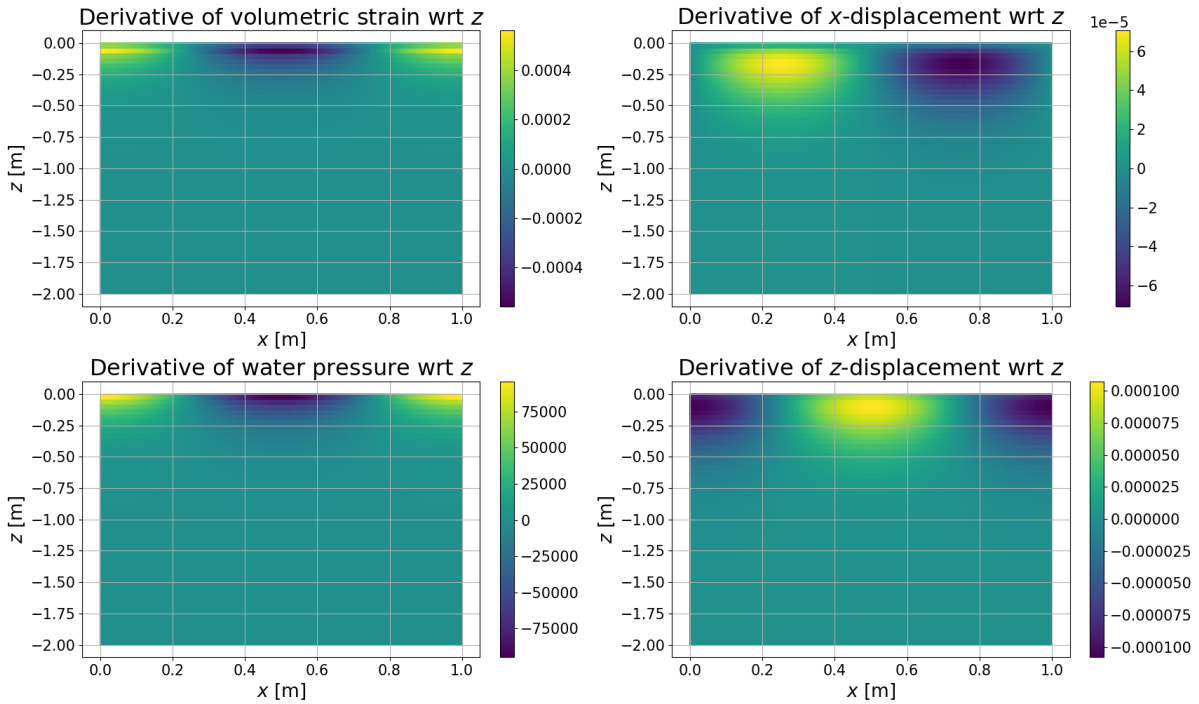

Figure 5.9: Derivatives of $\sigma'_{zz}, \epsilon_{\text{vol}}, P, u_x, u_z$ at $t = 92.25$s with respect to z, when water is assumed to be incompressible ($\beta = 5 \cdot 10^{-10}$) and the set of boundary conditions used is B-II.

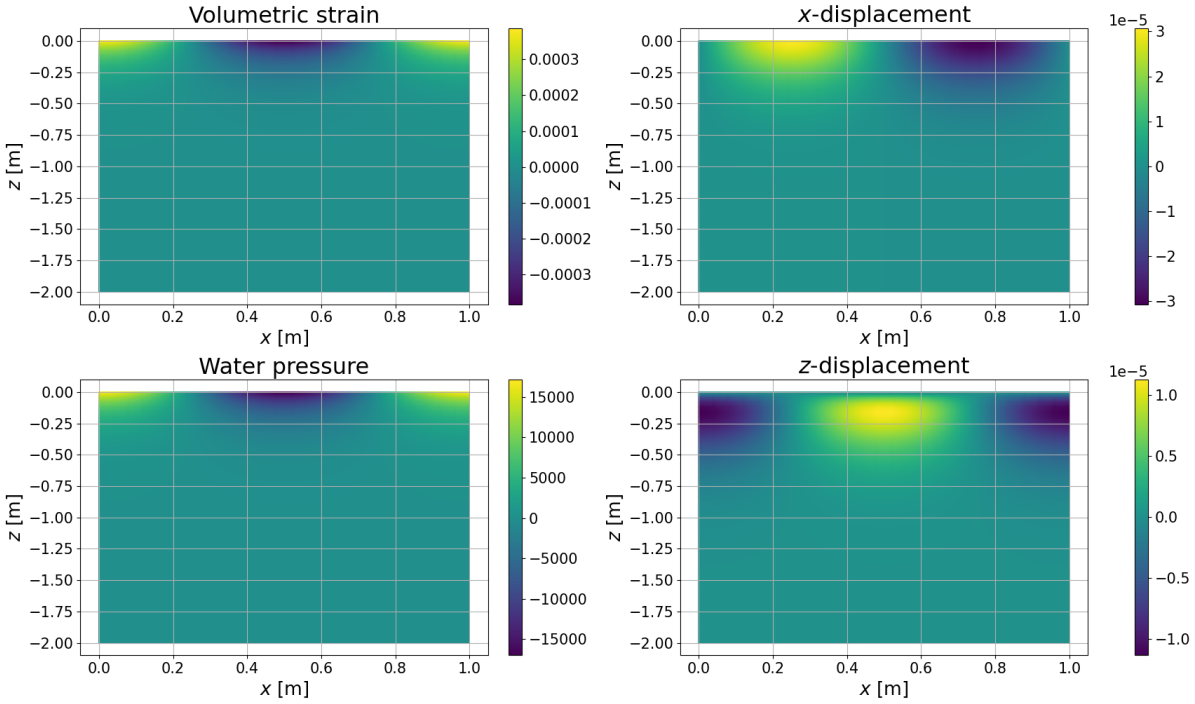

Figure 5.10: ϵ_{vol} [-], P [Pa], u_x [m] and u_z [m] at $t = 92.25$s, when water is assumed to be incompressible ($\beta = 5 \cdot 10^{-10}$) and the set of boundary conditions used is N-II.

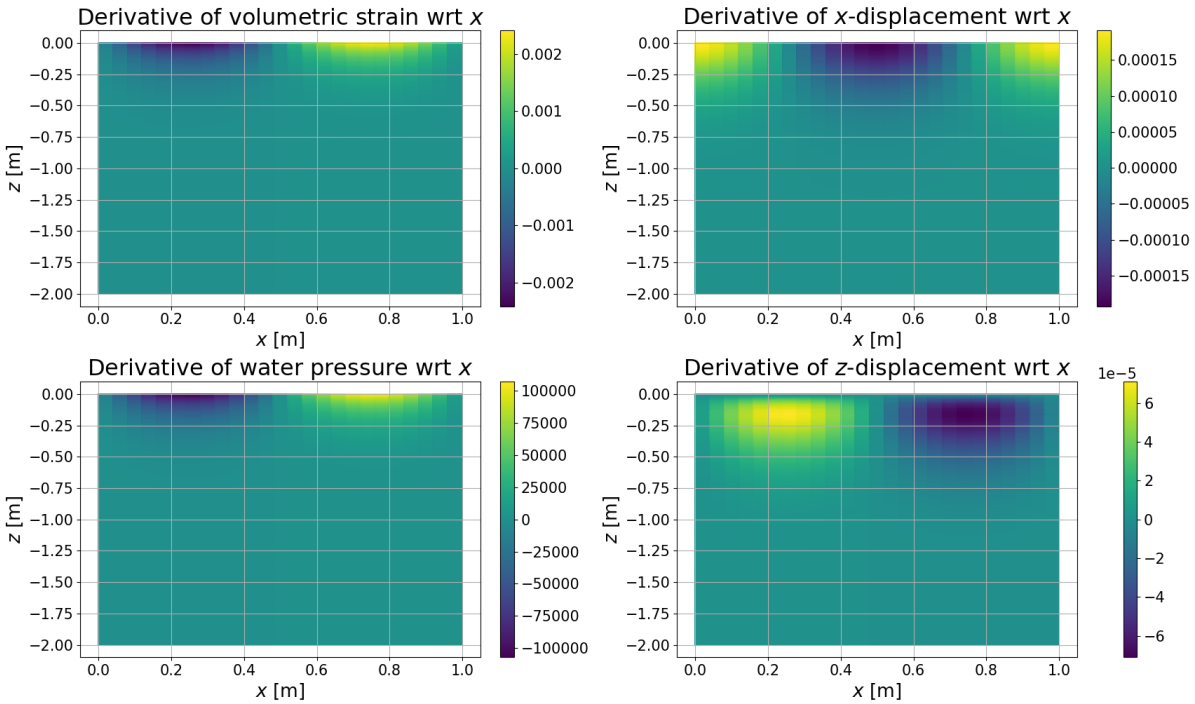

Figure 5.11: Derivatives of $\epsilon_{\text{vol}}, P, u_x, u_z$ at $t = 92.25$s with respect to x, when water is assumed to be incompressible ($\beta = 5 \cdot 10^{-10}$) and the set of boundary conditions used is N-II.

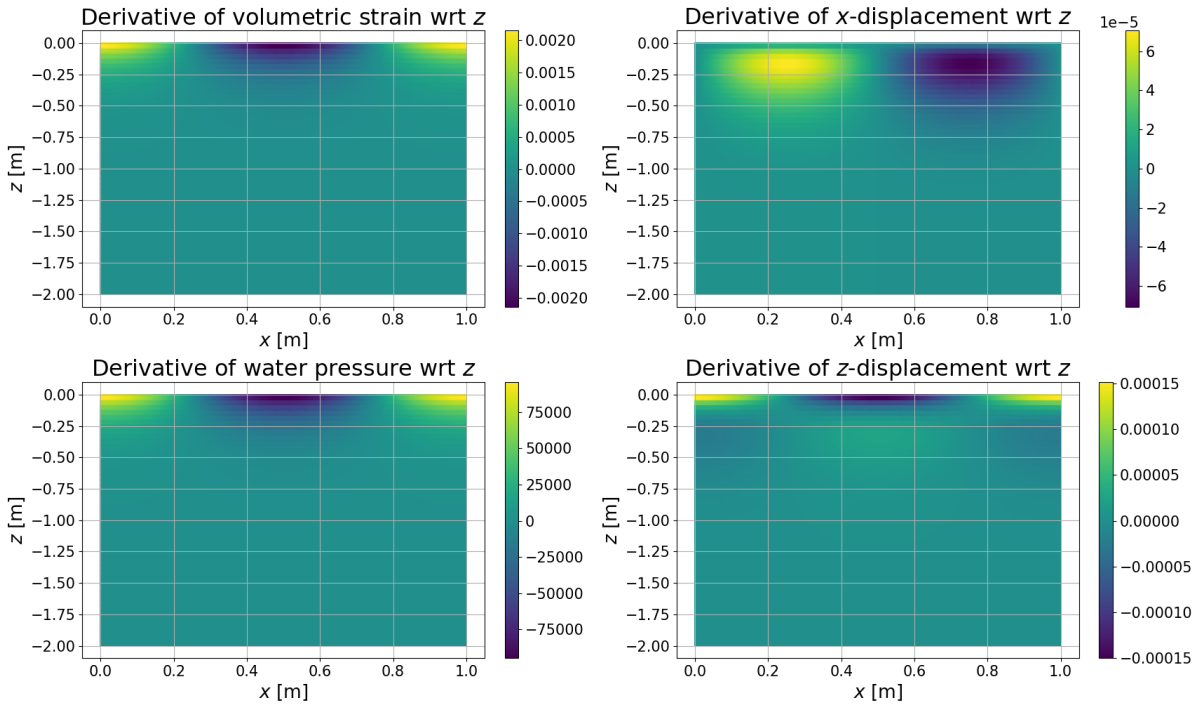

Figure 5.12: Derivatives of $\sigma'_{zz}, \epsilon_{\text{vol}}, P, u_x, u_z$ at $t = 92.25$s with respect to z, when water is assumed to be incompressible ($\beta = 5 \cdot 10^{-10}$) and the set of boundary conditions used is N-II.

6

Conclusions

The aim of this report was to extend the Msc thesis with two new situations for the computational domain in order to find the maximum difference between the model of Biot and the model of Van Damme & Den Ouden-Van der Horst. We came to the following conclusions based on this study.

	Model of Biot	**Model of Van Damme and Den Ouden-Van der Horst**
1.	Momentum balance equations are not satisfied.	Momentum balance equations are (approximately) satisfied.
2.	In one dimension, less boundary conditions for vertical displacement can be included.	In one dimension, more boundary conditions for vertical displacement can be included.
3.	In one dimension, we found a negative solution for the vertical displacement to Biots model, when the pore water pressure is positive.	In one dimensions, we found a positive solution for the vertical displacement to the new model, when the pore water pressure is positive.
4.	In this report we found that the following conclusion of our Msc thesis still holds: "The solution to the new model for the dynamic pore water pressure is similar to the solution to Biot's model. However, the solutions to the new model for the other variables as volumetric strain and displacements can differ significantly." This is especially true for the two-dimensional quicksand case, since then the behaviour of the vertical displacement for the new model is totally different from the vertical displacement for Biot's model. To know which behaviour is right, more research must be done for quicksand. The volumetric strain and displacement are hard to measure or can not be measured. Therefore, it is not possible yet to make a conclusion which model is best. However, we can verify that Biot's model and the new model can not only differ in value, but also in behaviour.	

Bibliography

[1] Klein, F. (2023a). Compressible vs. incompressible pore water in fully-saturated poroelastic soil: Msc thesis [Master's thesis, TU Delft and Rijkswaterstaat].

[2] Van Damme, M., & Den Ouden-Van der Horst, D. (2023). An alternative process-based approach to predicting the response of water saturated porous media to hydrodynamic loads. Journal of Porous Media. https://doi.org/10.1615/JPorMedia.2023045106

[3] Klein, F. (2023b). Compressible vs. incompressible pore water in fully-saturated poroelastic soil: Literature report [Master's thesis, TU Delft and Rijkswaterstaat].

[4] Liu, B., Jeng, D.-S., Ye, G., & Yang, B. (2015). Laboratory study for pore pressures in sandy deposit under wave loading. Ocean Engineering, 106, 207–219. https://doi.org/https://doi.org/10.1016/j.oceaneng.2015.06.029

[5] Verruijt, A. (2010). Soil mechanics.

B Two additional cases – November 1, 2024

Two additional cases on Msc thesis Compressible vs. incompressible water in poroelastic soil

Written for Deltares by ir. F.P.M. Klein

November 1, 2024

Contents

1

Introduction

This report is an extension on our MSc thesis last year [1]. In this report we will discribe two additional cases of boundary conditions for the model of Biot and the new model by Van Damme & Den Ouden-Van der Horst [2] for comparison between these two models in more detail.

In our literature report [3] and MSc thesis [1] we assumed that a positive pore water pressure is a pushing force and a negative pore water pressure is a pulling force. In Figure 1.1, the hydraulic load is denoted by the red arrows. Note that when the red arrow is pointing downwards there is a positive pressure on the soil (pushing force). On the other hand, when the red arrow is pointing upwards there is a negative pressure on the soil (pulling force) [1]. Furthermore, we have that the vorticity is zero everywhere on the domain.

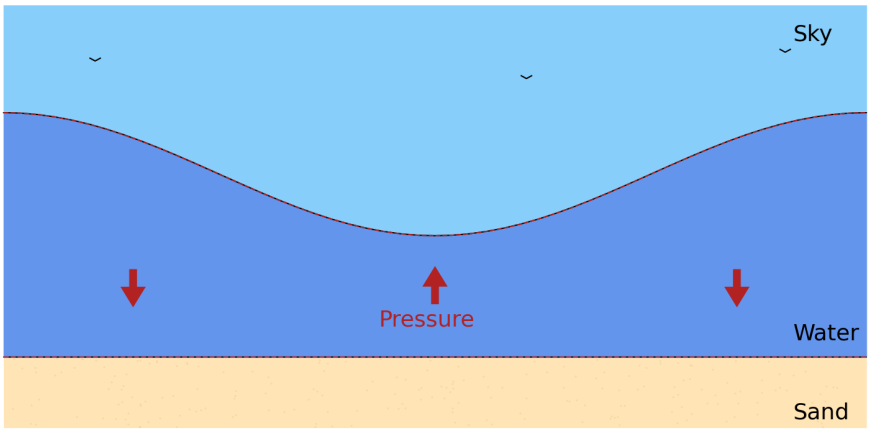

Figure 1.1: A flat foreshore subjected to water waves [1].

In Chapter 2 we will give a short recap of the two-dimensional governing equations for Biot's model in Section 2.1 and for the new model in Section 2.2. In Section 2.1.2 one additional case of boundary conditions for Biot's model is stated. In this case, the shear stress and the pore water pressure are set equal to zero at the top, while there is a pressure on the bottom. Furthermore, the effective stress is set equal to zero at the bottom. In Section 2.2.2 we will introduce two additional cases of boundary conditions for the two-dimensional new model. In the first case for the new model the normal effective stress and pore water pressure are set equal to zero at the top while there is pressure at the bottom. In the second case for both models the shear stress equal and pore water pressure are set to zero at the top while there is pressure at the bottom. Since we do not include gravity for these cases, we can flip this case along a horizontal line (so the top above becomes the bottom and vice versa) and reuse the calculation methods of our MSc thesis. In Section 2.3 we will describe the initial conditions. In Chapter 3 we will discuss the two-dimensional numerical results for Biot's model and the new model using the different sets of boundary conditions. Finally, in Chapter 4 we will make some conclusions.

2

Models (2D)

In the next sections we will take a look into the two-dimensional governing equations of Biot's model and the new model of Van Damme & Den Ouden-Van der Horst. Note that we have set the vorticity $\omega := \frac{\partial u_x}{\partial z} - \frac{\partial u_z}{\partial x}$ equal to zero [1].

2.1. Biot's model

In this section we will describe the two-dimensional governing equations of Biot's model and the corresponding set of boundary conditions.

2.1.1. Governing equations

It is common to describe Biot's model by three governing equations in two dimensions which are given by the conservation of mass equation and the momentum balance equation [1]. The conservation of mass equation in two dimensions is given by

$$\frac{\gamma_w}{K_s} p\beta \frac{\partial P}{\partial t} - \nabla^2 P + \frac{\gamma_w}{K_s} \frac{\partial}{\partial t}\left(\frac{\partial u_x}{\partial x} + \frac{\partial u_z}{\partial z}\right) = 0. \tag{2.1}$$

Respectively, the horizontal and vertical momentum balance equations are given by

$$-(\lambda + 2\mu)\nabla^2 u_x + \frac{\partial P}{\partial x} = 0, \tag{2.2}$$

$$-(\lambda + 2\mu)\nabla^2 u_z + \frac{\partial P}{\partial z} = 0. \tag{2.3}$$

To determine the volumetric strain we use the following equation

$$\epsilon = \frac{\partial u_x}{\partial x} + \frac{\partial u_z}{\partial z}. \tag{2.4}$$

2.1.2. Boundary conditions

In this section we will discuss the boundary conditions for the two-dimensional model of Biot. Most of the boundary conditions are from our MSc thesis [1].

In Biot's model it is common to set the total normal stress equal to the hydrodynamic load and to suppose that the normal effective stress equals zero which results in the water pressure being equal to the hydrodynamic load [3]. Then we set the boundary conditions $\sigma'_{zz} := -2\mu\frac{\partial u_z}{\partial z} - \lambda\epsilon_{\text{vol}} = 0$ and $P = F_{zz}(t)$ at $z = 0$, where $F_{zz}(t)$ represents the normal stress and only depends on time and is chosen to be positive [1]. The shear stress at the top is set equal to zero, i.e. $-\mu\left(\frac{\partial u_x}{\partial z} + \frac{\partial u_z}{\partial x}\right) = 0$

At the bottom, $z = -n_z$, we assume that the pore water pressure equals zero, i.e. $P = 0$. The shear stress is set equal to zero at the bottom by $u_z = \frac{\partial u_x}{\partial z} = 0$, because of stability issues for the numerical model of Biot. This way we had no stability issues which we got when we did not define a Dirichlet boundary condition for the horizontal displacement u_z at the bottom $z = -n_z$.

At $x = 0$ and $x = -n_x$ we get that $\frac{\partial u_z}{\partial x} = 0$, $u_x = 0$ and $\frac{\partial P}{\partial x} = 0$ [1].

Then we get that for Biot's model the sets of boundary conditions are given by

B-I

$$\text{for } z=0: \begin{cases} -\mu\left(\frac{\partial u_x}{\partial z}+\frac{\partial u_z}{\partial x}\right)=F_{xz} \\ P=F_{zz} \\ -\lambda\frac{\partial u_x}{\partial x}-(\lambda+2\mu)\frac{\partial u_z}{\partial z}=0 \end{cases}, \tag{2.5}$$

$$\text{for } z=-n_z: \begin{cases} u_z=\frac{\partial u_x}{\partial z}=0 \\ P=0 \end{cases}, \tag{2.6}$$

$$\text{and for } x=0 \text{ and } x=n_x: \begin{cases} u_x=\frac{\partial u_z}{\partial x}=\frac{\partial P}{\partial x}=0 \end{cases}, \tag{2.7}$$

Note that $-\lambda\frac{\partial u_z}{\partial z}-2\mu\epsilon_{\text{vol}}=0 \Longleftrightarrow -\lambda\frac{\partial u_x}{\partial x}-(\lambda+2\mu)\frac{\partial u_z}{\partial z}=0$, since $\epsilon_{\text{vol}}=\frac{\partial u_x}{\partial x}+\frac{\partial u_z}{\partial z}$.

Then we choose that [1]

$$F_{zz}(x,t)=0.5\gamma_w H\sin\left(2\pi\frac{t}{T}\right)\cos\left(2\pi\frac{x}{L}\right), \tag{2.8}$$

where γ_w [N/m^3] the specific weight of the pore water, H [m] is the wave height, L [m] the length of the wave, T [s] the wave period. On the other hand, when the pore water pressure at the bottom is zero, then there is no normal stress acting on the pore water particles and the total normal stress will only depend on the normal effective stress. This describes a case of uplift when flipped over a horizontal line.

2.2. New model

In this section we will describe the governing equations of the new model in two dimensions and the corresponding sets of boundary conditions..

2.2.1. Governing equations

In two dimensions, the model of Van Damme & Den Ouden-Van der Horst can be described by four governing equations, namely the equation for the pore water pressure (conservation of mass), the equation for the volumetric strain and the equation for displacement [2]. The derivation of these equations can be found in our master thesis [1]. The equation for the water pressure is given by

$$\frac{\gamma_w}{K_s}p\beta\frac{\partial P}{\partial t}-\nabla^2 P+\frac{\gamma_w}{K_s}\frac{\partial\epsilon_{\text{vol}}}{\partial t}=0. \tag{2.9}$$

The equation for the volumetric strain is given by

$$\frac{\gamma_w}{K_s}p\beta\frac{\partial P}{\partial t}-\nabla^2\epsilon_{\text{vol}}+\frac{\gamma_w}{K_s}\frac{\partial\epsilon_{\text{vol}}}{\partial t}=0. \tag{2.10}$$

The equation for the displacement in horizontal and vertical direction is given by

$$\frac{\partial^2 u_x}{\partial x^2}=\frac{\partial\epsilon_{\text{vol}}}{\partial x}, \tag{2.11}$$

$$\frac{\partial^2 u_z}{\partial z^2}=\frac{\partial\epsilon_{\text{vol}}}{\partial z}. \tag{2.12}$$

2.2.2. Boundary conditions

In this section we will discuss two sets of boundary conditions used for the new model in two dimensions. Both sets differ one boundary condition at the bottom $z=-n_z$. Most of the boundary conditions are from our MSc thesis [1].

In the new model we assume, like in Biot's model, that the pore water pressure equals the hydrodynamic load and that the shear stress is zero. However, we do not set the normal effective stress equal to zero [1]. In stead, the vertical momentum balance equation can be used again which is given by $-(\lambda+2\mu)\frac{\partial\epsilon_{\text{vol}}}{\partial z}+\frac{P}{\partial z}=0$ [2].

Then the sets of boundary conditions for the new model are given by [1]

N-I

$$\text{for } z=0: \begin{cases} -\mu\left(\frac{\partial u_x}{\partial z}+\frac{\partial u_z}{\partial x}\right)=F_{xz} \\ P=F_{zz} \end{cases}, \tag{2.13}$$

$$\text{for } z=-n_z: \begin{cases} -\lambda\frac{\partial u_z}{\partial z}-2\mu\epsilon_{\text{vol}}=0, \quad \text{which can be written as } u_x=\frac{\partial u_z}{\partial x}=0 \text{ if } P=0 \\ P=0 \end{cases}, \tag{2.14}$$

$$\text{and for } x=0 \text{ and } x=n_x: \begin{cases} u_x=\frac{\partial u_z}{\partial x}=\frac{\partial P}{\partial x}=0 \end{cases}, \tag{2.15}$$

N-II

$$\text{for } z=0: \begin{cases} -\mu\left(\frac{\partial u_x}{\partial z}+\frac{\partial u_z}{\partial x}\right)=F_{xz} \\ P=F_{zz} \end{cases}, \tag{2.16}$$

$$\text{for } z=-n_z: \begin{cases} -\mu\left(\frac{\partial u_x}{\partial z}+\frac{\partial u_z}{\partial x}\right)=F_{xz} \\ P=0 \end{cases}, \tag{2.17}$$

$$\text{and for } x=0 \text{ and } x=n_x: \begin{cases} u_x=\frac{\partial u_z}{\partial x}=\frac{\partial P}{\partial x}=0 \end{cases}, \tag{2.18}$$

We use the vertical momentum balance equation $-(\lambda+2\mu)\frac{\partial \epsilon_{\text{vol}}}{\partial z}+\frac{\partial P}{\partial z}=0$ for the volumetric equation at $z=0$ and/or $z=-n_z$, $\epsilon=\frac{\partial u_x}{\partial x}+\frac{\partial u_z}{\partial z}$ for the vertical displacement equation at $z=0$ and/or $z=-n_z$. Since these two conditions holds everywhere on the domain and are more like definitions, we use these as boundary conditions to solve the equations but are not 'new' boundary conditions and therefore not stated above.

2.3. Initial conditions

We assume that at the start, $t=0$, everything is at rest [3]. Therefore, no stresses act on the surface in the beginning which means that there are no stresses and displacements at time $t=0$ [2]. According to [1], this means that the volumetric strain and pressure must be zero too. Then we have that

$$u_z|_{t=0}=\epsilon_{\text{vol}}|_{t=0}=P|_{t=0}=0.$$

3

Numerical results (2D)

We will now look into the numerical results in two dimensions. For the numerical model in two dimensions we use the same methods as in our MSc thesis [1]. So we apply the Finite-Element Method to the models for discretisation in space and the Backward-Euler method for discretisation in time. The steps taken are described in our MSc thesis [1] in Chapter 4 and Section 5.1.1 for Biot's model, and Chapter 7 and Section 8.1.1 for the new model. We choose $n_z = 2$ and $n_x = 1$ which means that the computational domain becomes $[0, n_x] \times [-n_z, 0] = [0,1] \times [-2,0]$.

The values of the parameters are given by Tables 3.1, 3.2 and 3.3.

Table 3.1: Parameters of one layer of sandy deposit [4].

Soil properties	**Symbols**	**Values**
Hydraulic conductivity [m/s]	K_s	$1.8 \cdot 10^{-4}$
Porosity	p	0.425
Poisson ratio	υ_p	0.3
Shear modulus [Pa]	μ	$1.27 \cdot 10^{7}$
Specific weight of water [N/m^3]	γ_w	9810

Table 3.2: Parameters of compressibility equation given by $\beta = s\beta_0 + \frac{1-s}{P_0}$.

Soil properties	**Symbols**	**Values**
Degree of saturation [4]	s	1.0
Compressibility of pure water [5]	β_0	$0.5 \cdot 10^{-9}$
Absolute pressure in the water [Pa] [5]	P_0	10^5

Table 3.3: Parameters of the waves [4].

Wave properties	**Symbols**	**Values**
Wave period [s]	T	9
Wave height [m]	H	3.5
Wave length [m]	L	n_x

3.1. Biot's model

Using boundary conditions B-I for Biot's model, we find the results shown in Figures 3.1, 3.2 and 3.3. Then we find that all boundary conditions of B-I hold. Note that the volumetric strain behaves a bit different than we expect. It is not following the behaviour of the water pressure at $z = 0$. However, we noticed that when we set $\frac{\partial u_x}{\partial z} = 0$, we do find the same behaviour for the volumetric strain and water pressure. Note that by setting the shear stress to zero and having the vorticity to be zero everywhere on the domain, we get that $\frac{\partial u_x}{\partial z} = 0$. This difference is also shown in our MSc thesis [1]. Therefore, we will also show the results for the boundary conditions B-I with the shear stress boundary condition replaced by $\frac{\partial u_x}{\partial z} = 0$. We will call this new set of boundary conditions B-II. This is shown in Figures 3.4, 3.5 and 3.6. We also noticed that the boundary conditions B-I (and B-II) were the only boundary conditions that describe similar behaviour as boundary conditions N-I and N-II and gave stable results (all boundary conditions met and no results going to infinity). Lastly, note that the momentum balance equations do not hold for Biot's model.

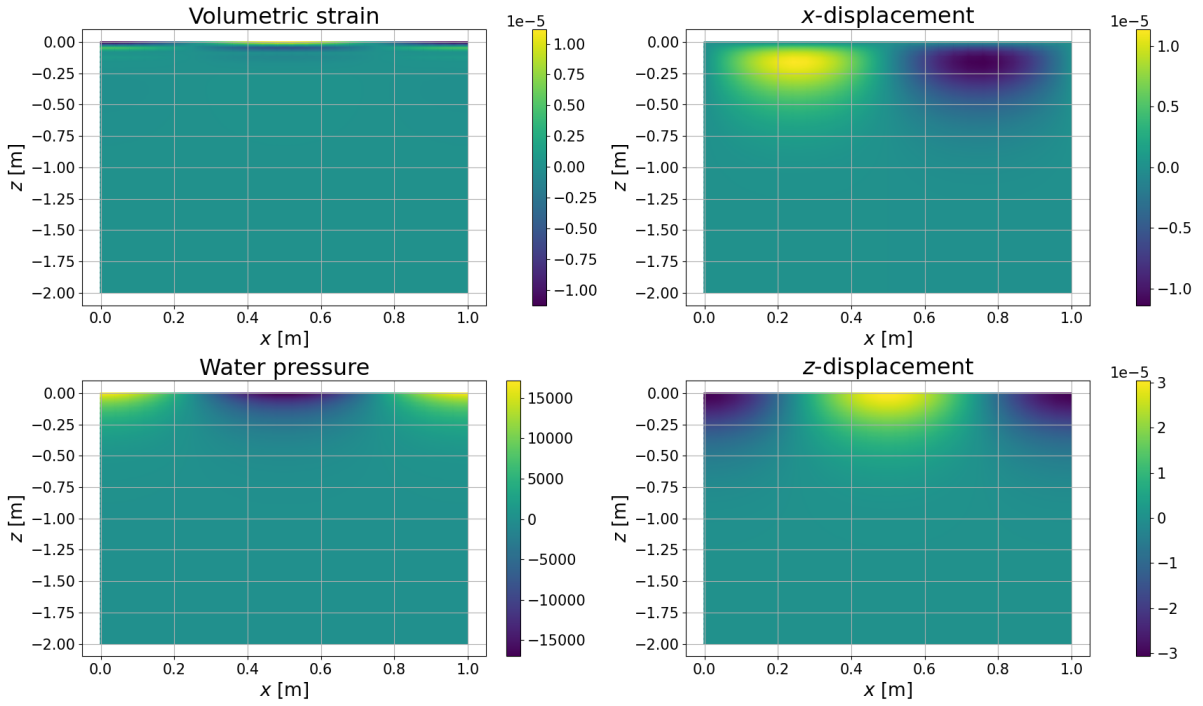

Figure 3.1: ϵ_{vol} [-], P [Pa], u_x [m] and u_z [m] at $t = 92.25$s, when water is assumed to be incompressible ($\beta = 5 \cdot 10^{-10}$) and the set of boundary conditions used is B-I.

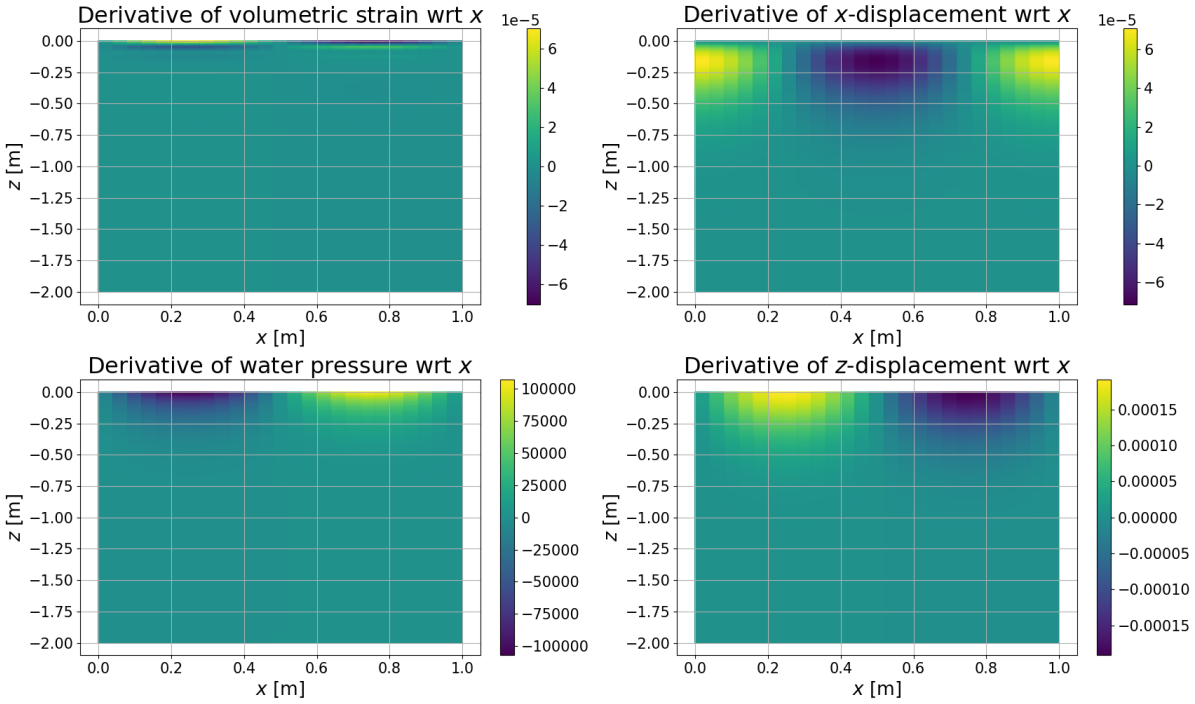

Figure 3.2: Derivatives of $\epsilon_{\text{vol}}, P, u_x, u_z$ at $t = 92.25$s with respect to x, when water is assumed to be incompressible ($\beta = 5 \cdot 10^{-10}$) and the set of boundary conditions used is B-I.

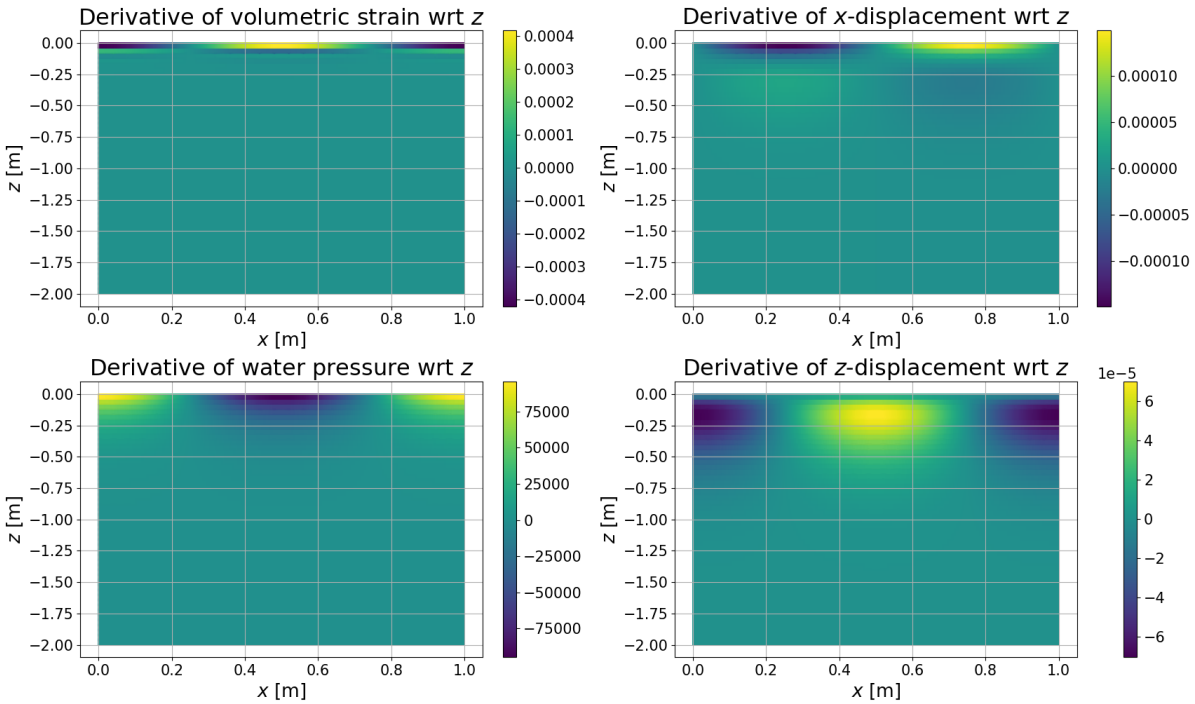

Figure 3.3: Derivatives of $\epsilon_{\text{vol}}, P, u_x, u_z$ at $t = 92.25$s with respect to z, when water is assumed to be incompressible ($\beta = 5 \cdot 10^{-10}$) and the set of boundary conditions used is B-I.

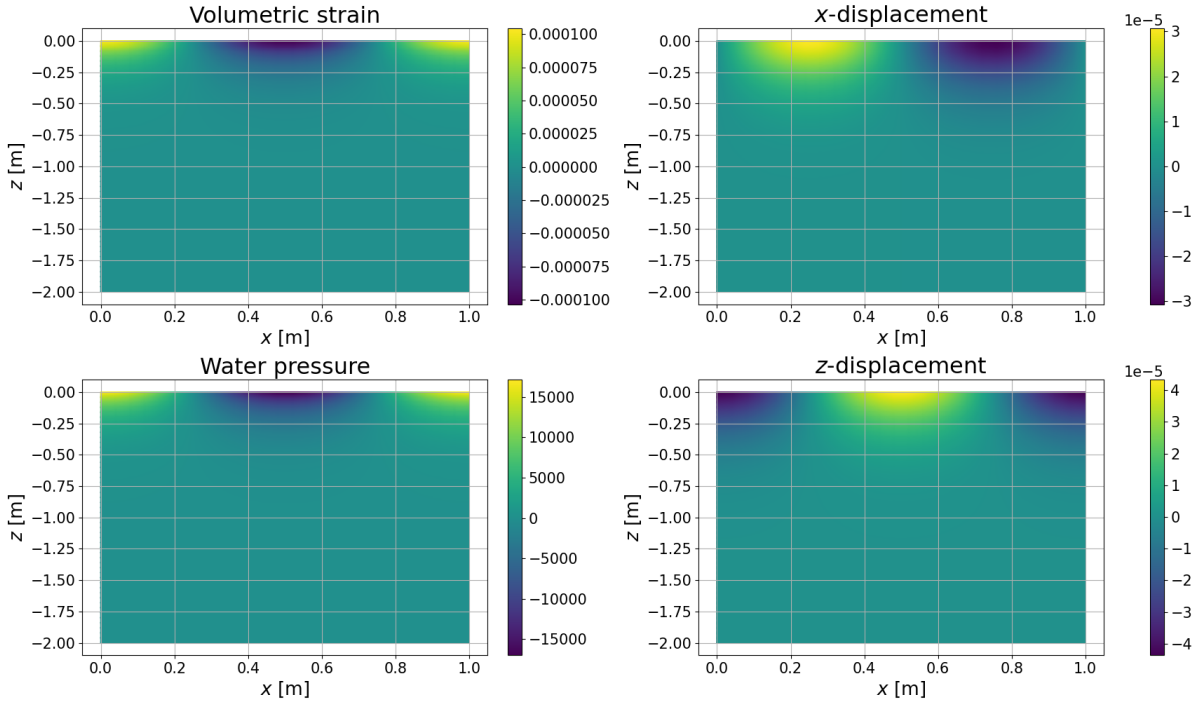

Figure 3.4: ϵ_{vol} [-], P [Pa], u_x [m] and u_z [m] at $t = 92.25$s, when water is assumed to be incompressible ($\beta = 5 \cdot 10^{-10}$) and the new set of boundary conditions used is B-II.

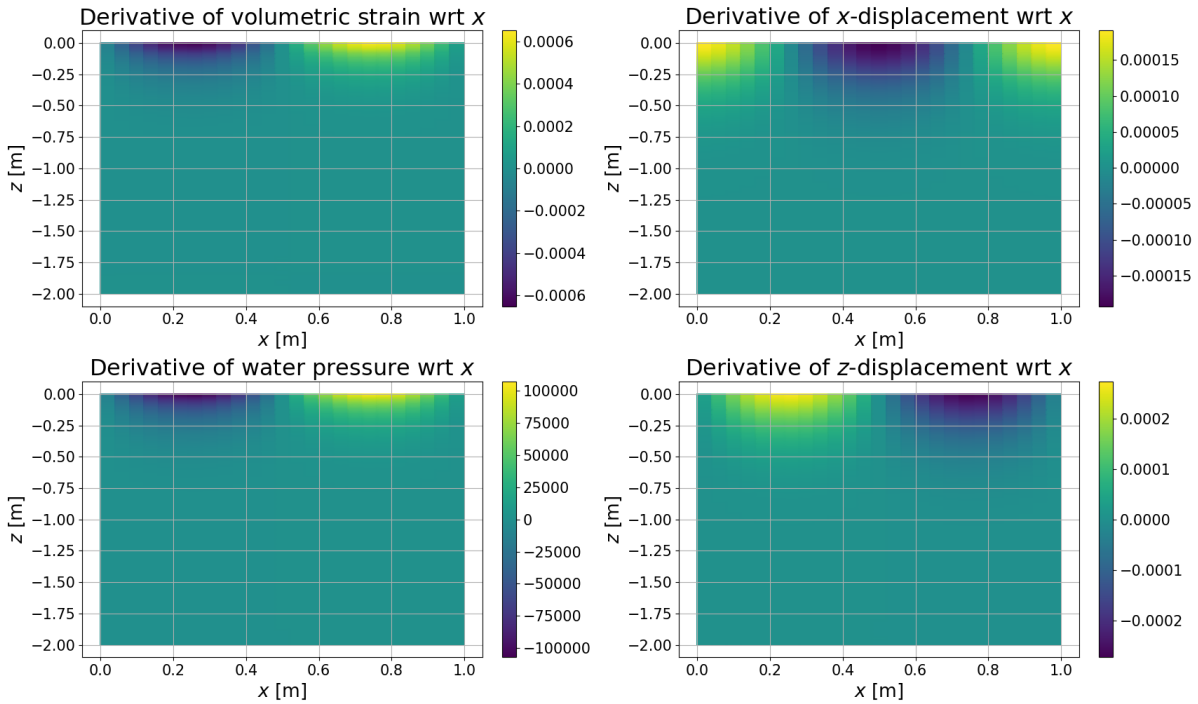

Figure 3.5: Derivatives of $\epsilon_{vol}, P, u_x, u_z$ at $t = 92.25$s with respect to x, when water is assumed to be incompressible ($\beta = 5 \cdot 10^{-10}$) and the new set of boundary conditions used is B-II.

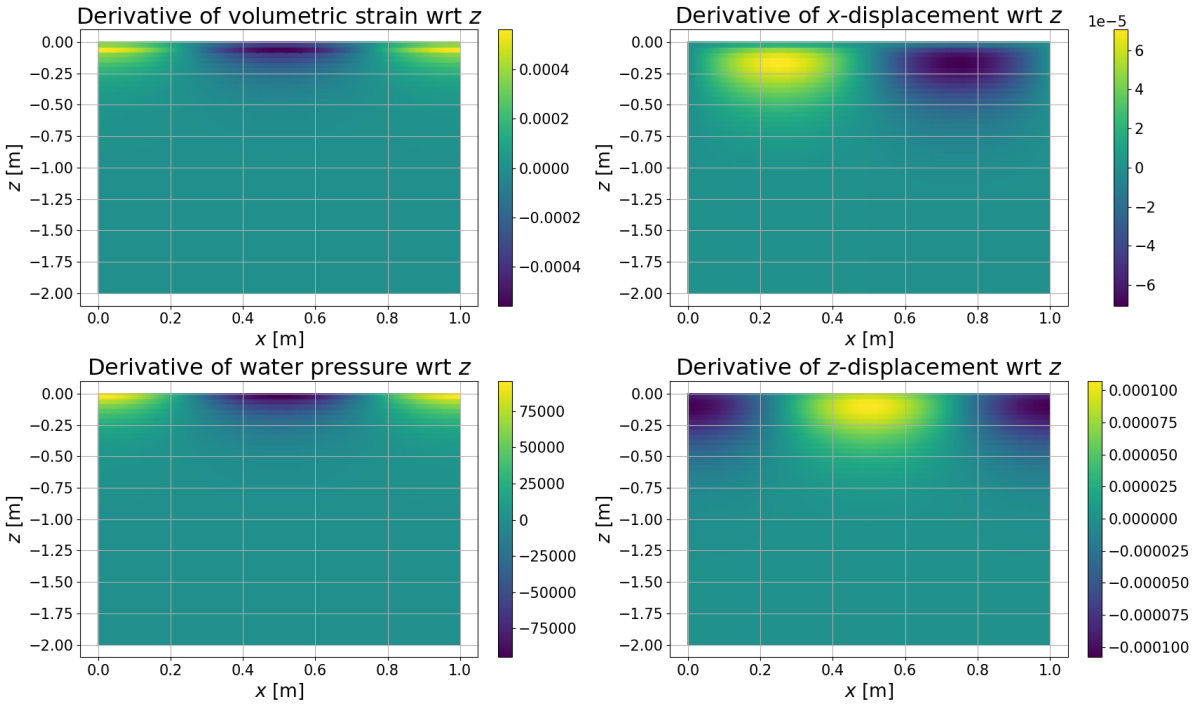

Figure 3.6: Derivatives of $\epsilon_{\text{vol}}, P, u_x, u_z$ at $t = 92.25$s with respect to z, when water is assumed to be incompressible ($\beta = 5 \cdot 10^{-10}$) and the new set of boundary conditions used is B-II.

3.2. New model

- When using boundary conditions N-I for the new model, we find the results shown in Figures 3.7, 3.8 and 3.9. Then we noticed that all boundary conditions of N-I hold. Note that also the momentum balance equations hold for the new model with N-I. Furthermore, we find that the volumetric strain times the constant $(\lambda + 2\mu)$ equals the water pressure, since we implemented the new model like in Section 8.1.1 of our MSc thesis [1]. Therefore, we also find that the volumetric strain follows the behaviour of the pore water pressure and is more than times larger than the case B-I for Biot's model. For the new model with N-I we find that the horizontal displacement is about three times as large and that the vertical displacement is about three times smaller than for Biot's model with B-I.

  When we compare the results of the new model with N-I to the results of Biot's model with B-II, we find that the solutions for the volumetric strain, water pressure and displacements behaves similar for both models. However, the volumetric strain is about four times larger, the vertical displacement about four times smaller for the new model with N-I than for Biot's model with B-II. The horizontal displacements are about the same. Lastly, we find that when changing 'the shear stress being equal to zero' to 'the derivative of the horizontal displacement with respect to z being equal to zero' did not make a noticeable difference.

- When using boundary conditions N-II for the new model, we find the results shown in Figures 3.10, 3.11 and 3.12. Then we find that all boundary conditions of N-II hold. We find that the volumetric strain follows the behaviour of the pore water pressure and is again more than then times larger than the case B-I for Biot's model. For the new model using N-II we find that the horizontal displacement is about two times larger and that the vertical displacement is about two times smaller than for Biot's model using boundary conditions B-I.

  When we compare the results of the new model with N-II to the results of Biot's model with B-II, we find that the solution for the volumetric strain behaves similar for both models, but the volumetric strain is about four times larger for the new model than for Biot's model. The solution for the horizontal displacement of both models behaves similar, but the solution of the new model with N-II is about two-third of the solution of Biot's model with B-II. The solution for the vertical displacement behaves also similar for both models but it is more than two times smaller for the new model with N-II than for

Biot's model with B-II. Lastly, we find that when changing $\sigma'_{zz} = 0$ to $\frac{\partial u_x}{\partial z} = 0$ did not make a noticeable difference.

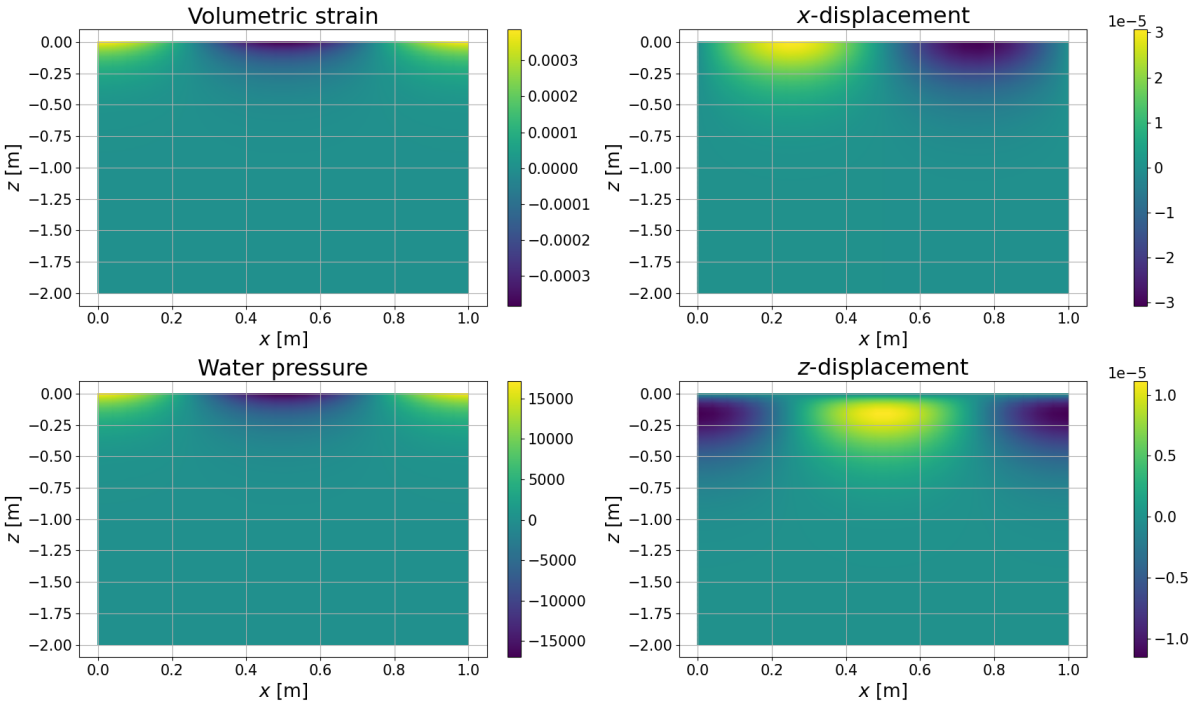

Figure 3.7: ϵ_{vol} [-], P [Pa], u_x [m] and u_z [m] at $t = 92.25$s, when water is assumed to be incompressible ($\beta = 5 \cdot 10^{-10}$) and the set of boundary conditions used is N-I.

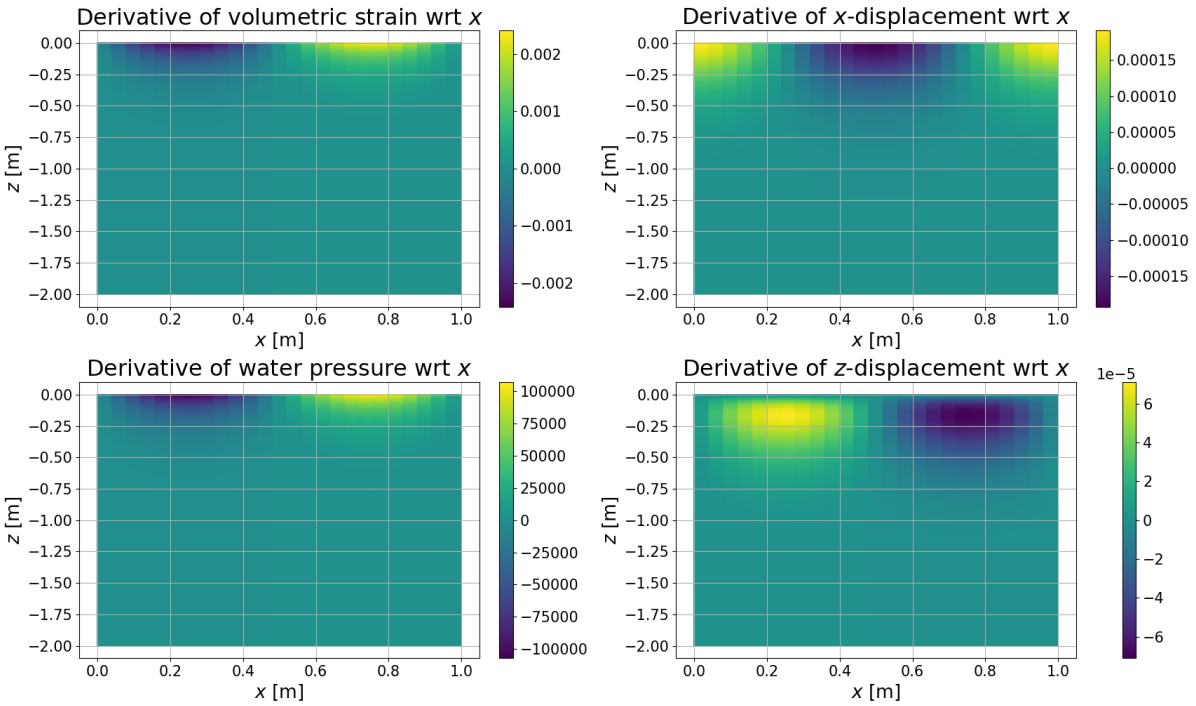

Figure 3.8: Derivatives of $\epsilon_{\text{vol}}, P, u_x, u_z$ at $t = 92.25$s with respect to x, when water is assumed to be incompressible ($\beta = 5 \cdot 10^{-10}$) and the set of boundary conditions used is N-I.

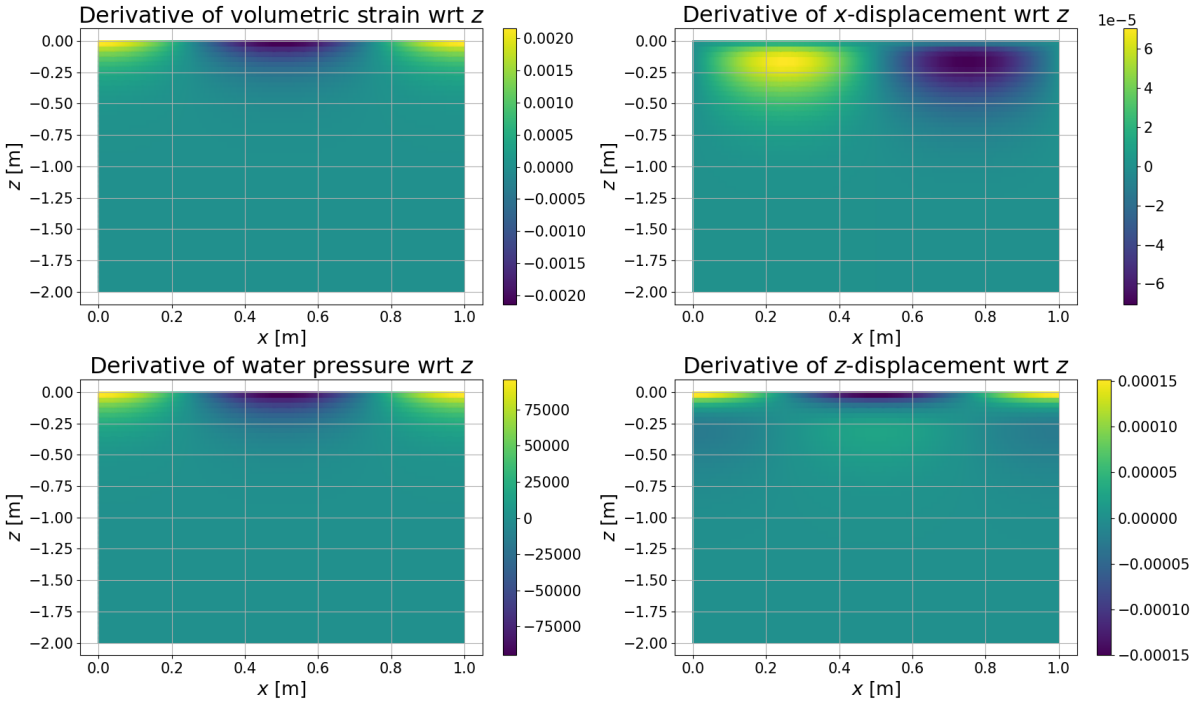

Figure 3.9: Derivatives of $\epsilon_{\text{vol}}, P, u_x, u_z$ at $t = 92.25$s with respect to z, when water is assumed to be incompressible ($\beta = 5 \cdot 10^{-10}$) and the set of boundary conditions used is N-I.

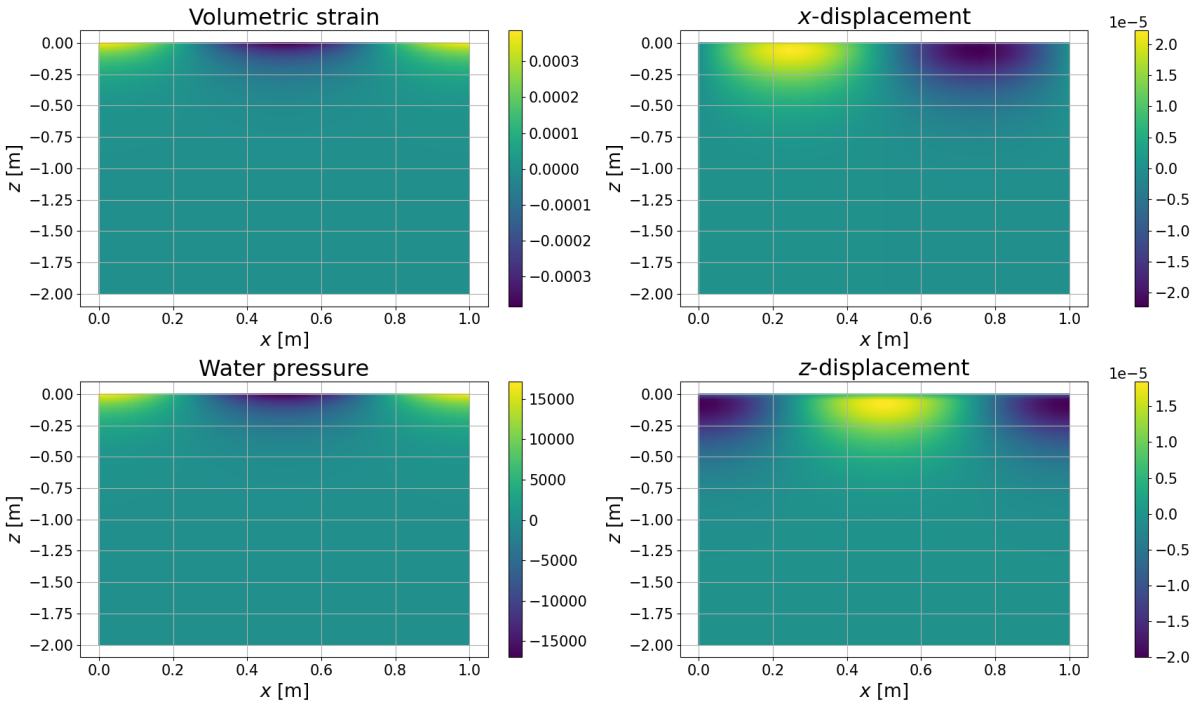

Figure 3.10: ϵ_{vol} [-], P [Pa], u_x [m] and u_z [m] at $t = 92.25$s, when water is assumed to be incompressible ($\beta = 5 \cdot 10^{-10}$) and the set of boundary conditions used is N-II.

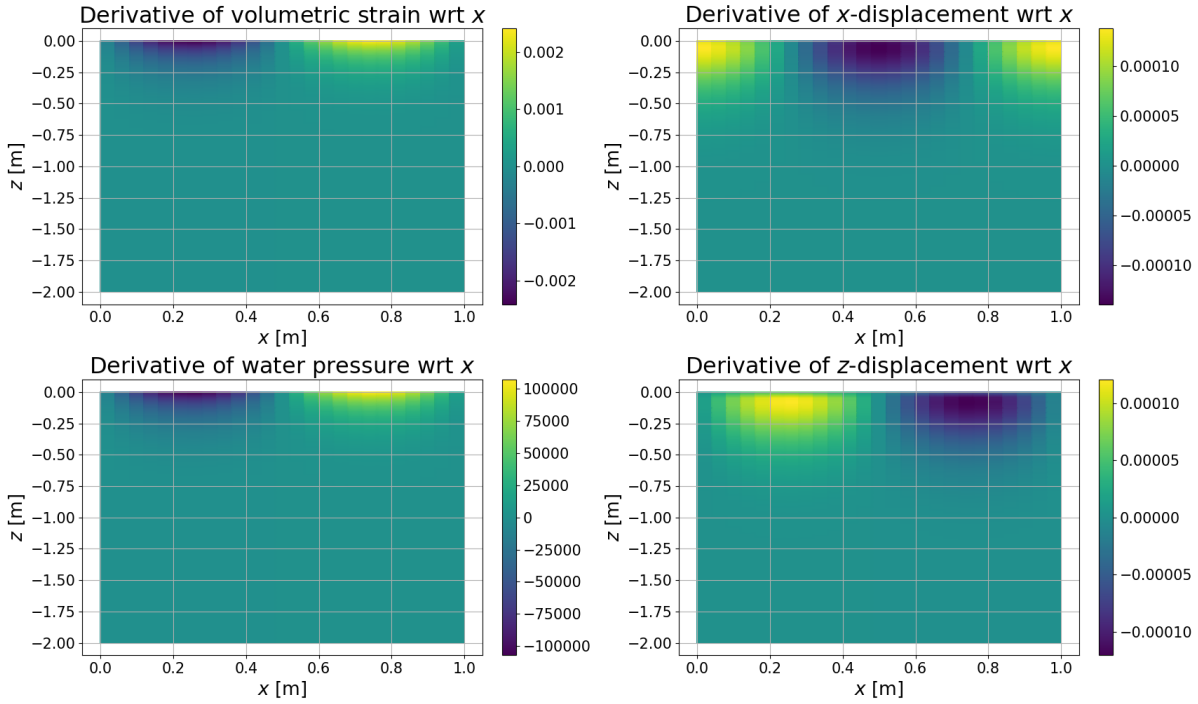

Figure 3.11: Derivatives of $\epsilon_{\text{vol}}, P, u_x, u_z$ at $t = 92.25$s with respect to x, when water is assumed to be incompressible ($\beta = 5 \cdot 10^{-10}$) and the set of boundary conditions used is N-II.

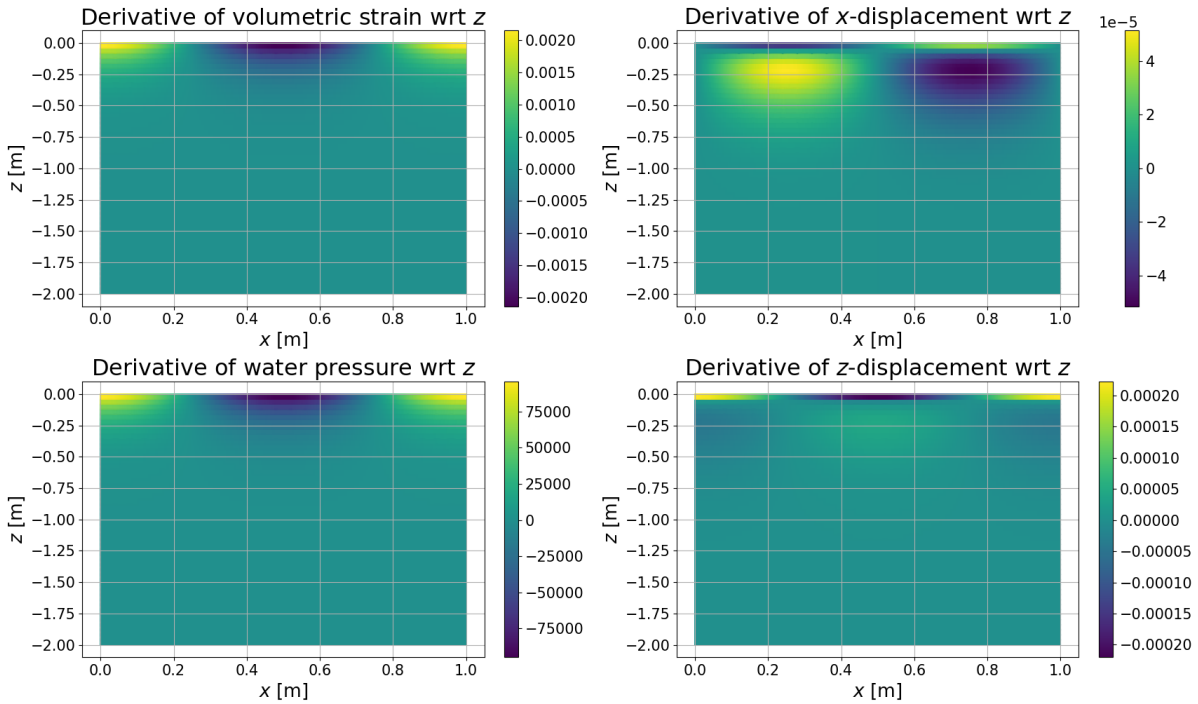

Figure 3.12: Derivatives of $\epsilon_{\text{vol}}, P, u_x, u_z$ at $t = 92.25$s with respect to z, when water is assumed to be incompressible ($\beta = 5 \cdot 10^{-10}$) and the set of boundary conditions used is N-II.

4

Conclusions

The aim of this report was to extend the MSc thesis with two new situations for the computational domain in order to find the maximum difference between the model of Biot and the model of Van Damme & Den Ouden-Van der Horst. We came to the following conclusions based on this study.

	Model of Biot	**Model of Van Damme and Den Ouden-Van der Horst**
1.	Momentum balance equations are not satisfied.	Momentum balance equations are (approximately) satisfied.
2.	The numerical version of Biot's model is less stable than the numerical version of the new model.	The numerical version of the new model looks quite stable. More different boundary conditions can be set than for Biot.
3.	All cases of Biot's model and the new model describe an uplift of a layer with pressure on the bottom, but have different boundary conditions at the top. In the methods we used, these cases were flipped along a horizontal line, since there is no gravity assumed. After comparing these cases of Biot's model and the new model we found that the following conclusion of our MSc thesis still holds: "The solution to the new model for the dynamic pore water pressure is similar to the solution to Biot's model. However, the solutions to the new model for the other variables as volumetric strain and displacements can differ significantly." Since the volumetric strain and displacement are hard to measure or can not be measured and the numerical models can be a bit unstable, it is not possible yet to make a conclusion which model is best. Therefore, more research must be done.		

Bibliography

[1] Klein, F. (2023a). Compressible vs. incompressible pore water in fully-saturated poroelastic soil: Msc thesis [Master's thesis, TU Delft and Rijkswaterstaat].

[2] Van Damme, M., & Den Ouden-Van der Horst, D. (2023). An alternative process-based approach to predicting the response of water saturated porous media to hydrodynamic loads. Journal of Porous Media. https://doi.org/10.1615/JPorMedia.2023045106

[3] Klein, F. (2023b). Compressible vs. incompressible pore water in fully-saturated poroelastic soil: Literature report [Master's thesis, TU Delft and Rijkswaterstaat].

[4] Liu, B., Jeng, D.-S., Ye, G., & Yang, B. (2015). Laboratory study for pore pressures in sandy deposit under wave loading. Ocean Engineering, 106, 207–219. https://doi.org/https://doi.org/10.1016/j.oceaneng.2015.06.029

[5] Verruijt, A. (2010). Soil mechanics.

Deltares is an independent institute for applied research in the field of water and subsurface. Throughout the world, we work on smart solutions for people, environment and society.

Deltares

www.deltares.nl